CHAPTER 7

CAVITATION

7.1 Introduction

The term *cavitation* was first used by R.E. Froude, S.W. Barnaby and Sir Charles Parsons in connection with propeller performance breakdown of early steamships. In 1895 Parsons built the first water tunnel to study cavitation, and some 20 years later he made the connection between cavitation and the erosion of marine propellers.

Cavitation is the rupture of a liquid or of a liquid-solid interface caused by reduction of local static pressure. A *rupture* is the formation of a macroscopic or visible bubble. Liquids contain many microscopic and submicroscopic voids which, as will be explained, act as *nuclei* for cavitation. However, cavitation is only said to occur when these voids grow to significant size. Cavitation is distinguished from boiling in being caused by a reduction of local static pressure rather than by an increase of temperature.

Cavitation occurs in many ways, can have both beneficial and deleterious effects, produces light as well as sound and is of interest to physicists, chemists, biologists and doctors as well as to many types of engineers. Controlled cavitation is used in the ultrasonics industry for cleaning, etching and cutting. It is also used to accelerate some chemical reactions, and it may be used in the practice of medicine for destruction of undesirable cells. However, most interest in cavitation is in avoiding its undesired effects. Not only does cavitation produce unwanted noise, but also it causes erosion damage to pipes, valves, pumps, turbines and propellers. It also causes damage in bearings, contributes to erosion of diesel-engine cylinder liners and limits the outputs of sonar transducers.

Cavitation is an especially important noise source in underwater acoustics. Since it involves volume changes, it is basically a monopole noise source. In marine vehicles, cavitation usually occurs most seriously on the propulsor. While submarines and torpedoes can often avoid cavitation by operating at deep depths, surface ships cannot avoid it. Propeller cavitation noise of surface ships is usually dominant over the entire spectrum from subaudible to ultrasonic frequencies; whenever submarines or torpedoes operate so as to experience cavitation, it is a dominant noise source for them as well.

Cavitation is described by the *cause* of the static pressure drop, the *location* of the rupture and the *contents* of the bubble. One cause of cavitation is the pressure drop occurring in the negative half cycle of a sound wave. A sound wave in a liquid having a sound pressure level (SPL) of 220 dB re 1 μPa has a peak negative pressure of over 1 atm. Such *acoustic cavitation* can limit transducer outputs but also is used to produce beneficial effects in ultrasonics devices. A second cause of pressure drop is flow of liquids in hydraulic systems, called *hydraulic cavitation*. A third type is associated with the motion of bodies in a liquid, or the equivalent motion of liquids past stationary bodies. This is termed *body cavitation* for three-dimensional bodies and *hydrofoil cavitation* for flows past two-dimensional shapes. Since they experience the highest relative flow

speeds, propeller blade tips are usually the first part of a vehicle to cavitate. *Propeller cavitation* is a most important source of underwater noise.

There are two locations where cavitation occurs: at a liquid-solid interface or within the volume of the liquid. While theory usually deals with *volume cavitation*, most cavitation actually occurs at or very close to solid surfaces, as *boundary* or *surface cavitation*.

All cavitation bubbles contain mixtures of vapor and gas, and cavitation is called vaporous or gaseous depending on which is dominant. *Vapor cavitation* causes most of the noise and erosion associated with cavitation, but *gaseous cavitation* can limit transducer outputs and cause serious effects in biological systems.

Robertson (1969) estimated that more than 10,000 papers have been published on cavitation, yet there are only a very few books devoted to this subject, most of which are the proceedings of symposia. Similarly, the subject is often mentioned in university courses but rarely treated in any detail. This lack of attention is hard to comprehend. The present chapter covers the physics of this phenomenon, with emphasis on those aspects important to an understanding of its noise production. The following chapter covers propeller cavitation and includes sections on surface ship noise and the contribution of such noise to the ocean's ambient background.

7.2 Tensile Strength of Liquids

A *fluid* is distinguished from a solid by the fact that it cannot permanently sustain a shear stress. Most persons would describe a *liquid* as an almost incompressible fluid that cannot sustain tension. Actually the latter attribute is not always true. Under certain conditions liquids can sustain very high tensions without rupturing. In fact, very pure liquids are capable of withstanding tensions of tens or even hundreds of atmospheres. It is impurities in a liquid that cause it to rupture at much lower pressures.

Static Tensile Strength

The intermolecular forces resisting rupture of a pure, gas-free liquid are very strong. Calculations based on the kinetic theory of liquids predict static tensile strengths for water in excess of a thousand atmospheres. Other estimates, based on the van der Waals equation of state, predict maximum strengths of the order of 250 to 275 atm. Attempts at measurement within the volume of a liquid are often frustrated by ruptures at liquid-solid interfaces. However, several investigators have observed values in excess of 100 atm.

Extremely high tensions have only been measured with small samples of very pure liquid in very clean containers. However, tensions of up to an atmosphere or so can occur in the laboratory without such extreme measures. All that is required is that prior to the experiment the liquid be pressurized or other steps taken to eliminate undissolved air bubbles. It is this ability of water free of entrapped air to sustain tension that is responsible for boiler explosions. When water has been boiled for a long time, it may lose its air bubbles and be able to sustain several degrees of superheat. When this happens, each rupture releases a lot of energy. A crack may then occur, followed by an explosion.

Cavitation Nuclei

It is now recognized that the seeds of cavitation and boiling are the many small impurities and/or microscopic bubbles that normally exist in a liquid. To understand how these nuclei control cavitation inception, consider a small, gas-filled, spherical void in a liquid. Because of the

action of surface tension, the pressure inside the bubble is higher than that outside. Thus, the pressure outside the bubble can be reduced somewhat below zero, i.e., can become a tension, while the pressure inside the bubble remains positive. If the outside pressure is reduced below zero by an amount that exceeds the surface-tension pressure rise, then the pressure inside the bubble will be low enough that rapid vaporization can take place and rupture will occur.

The pressure drop across a stationary free surface due to surface tension is given by

$$\Delta p = p_i - p_o = \frac{2\sigma}{a} , \tag{7.1}$$

where σ is the surface tension and a is the radius of curvature of the surface. For water at room temperature, $\sigma \doteq 72$ dynes/cm. Figure 7.1 is a plot of the surface-tension pressure change as a function of radius, showing, for example, that a radius of 10^{-4} cm will sustain a pressure difference of 1.4 atm. Static tensions of over 100 atm. require that maximum bubble sizes be under 10^{-6} cm, i.e., so small as not to be visible under a powerful microscope.

While today there is no doubt that nuclei control cavitation inception, there is still considerable controversy in the literature concerning the exact nature of the nuclei and their causes. Akulichev (1965, 1966) has considered the roles of solid particles and of ions. He found that ions causing negative hydration reduce the tensile strength of water, while positive hydration ions have no effect. Apfel (1970) has explained experimental results of Strasberg (1959), Barger (1964),

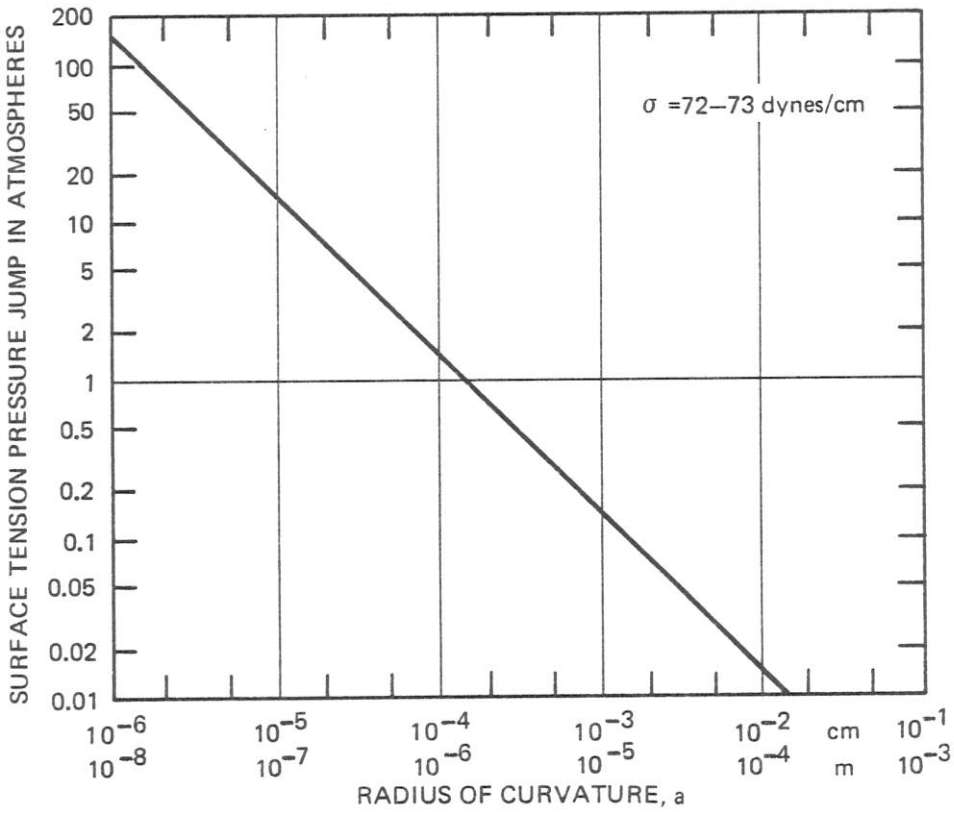

Fig. 7.1. Surface-Tension Pressure Difference Across a Water Surface as Function of Curvature

Galloway (1954) and others by assuming nuclei to be gas-filled crevices in tiny solid motes. Bernd (1966) considered the effects of surface films in stabilizing such nuclei. Sette and Wanderlingh (1962) showed that even cosmic rays can affect the nucleus population in a pure liquid. Sirotyuk (1965) has shown that tensile strength is clearly related to the distribution of nuclei, as has Lauterborn (1969) who found that repeated cavitation tends to use up the largest nuclei and that tensile strength therefore increases with time.

In summary, although the exact cause and nature of submicroscopic nuclei in liquids are uncertain, there is full agreement that somehow such gas nuclei do exist, and that the largest ones in a population determine the tensile strength of the liquid.

Dynamic Tensile Strengths

Often, as in flowing liquids or in exposure to transient pulses, the liquid is under tension for only a short time. In such cases higher breaking strengths are found, either because the largest nuclei happen not to be in the peak negative-pressure region or because there is insufficient time for a microscopic bubble to grow into a macroscopic one. Many researchers have reported on cavitation inception experiments in a variety of liquids with a number of different types of setups. It is generally agreed that dynamic effects can be important when exposure times are shorter than about 1 msec.

Dynamic effects are especially important in ultrasonics, where exposure times per cycle are less than 0.03 msec. They are also important in many laboratory experiments, such as water tunnel tests, for which exposures of less than 1 msec are common. However, most full-scale marine occurrences involve exposure times in excess of 10 or even 100 msec, providing ample time for macroscopic cavities to form. Also, most liquids encountered in engineering situations are relatively dirty and contain numerous nuclei larger than 10^{-3} cm. Thus, it is only in model experiments and in ultrasonics that liquids sustain tension. Liquids in most practical situations break as soon as the local static pressure drops to vapor pressure, if not sooner.

7.3 Single Bubble Growth and Collapse

A cavitation nucleus subjected to sufficient tension to cause the inside pressure to drop to the vapor pressure will expand as a vapor bubble until it experiences a positive pressure, at which point it will cease growing, will reverse the procedure and collapse. A number of phenomena affect the rates of growth and collapse, different ones being important for different phases of the growth-collapse cycle. These include pressure and velocity fields of a moving boundary, surface tension, evaporation, heat conduction, viscosity and compressibility. A complete equation including all of these effects would not only be non-linear but would also be so complex that understanding of the physics would be lost. It would not show clearly how different effects are dominant during different phases of the process. Thus, heat conductivity is important in the initial stage of growth of bubbles in boiling but has little effect in cavitation except sometimes during the final stages of collapse. Compressibility can become important in the final stages of collapse if bubble wall speeds approach the speed of sound, but not otherwise. Viscosity plays a role in inception, and may do so again in final collapse.

However, except for the periods when cavity growth is initiated and when final collapse occurs, the two dominant effects are the interaction of the velocity and pressure fields of a moving surface. These are the basis of classical theory of cavitation dynamics which can therefore be very useful even though it ignores the other, less important effects.

Classical Theory

Classical theory of bubble dynamics treats a uniformly expanding spherical surface in an ideal incompressible medium. The velocity potential for such a surface, as derived by Lamb (1932), is given by

$$\Phi = \frac{a^2 \dot{a}}{r} , \tag{7.2}$$

where a is its instantaneous radius. The equation of motion (Eq. 2.43 of Section 2.2) can be written in terms of the velocity potential. For an irrotational motion of an incompressible fluid, the result is

$$grad \left(\frac{p}{\rho_o} + \frac{1}{2} (\nabla \Phi)^2 - \frac{\partial \Phi}{\partial t} \right) = 0 . \tag{7.3}$$

Hence, for an expanding sphere,

$$\frac{p(r)}{\rho_o} + \frac{1}{2} \left(\frac{a^2 \dot{a}}{r^2} \right)^2 - \left(\frac{2a\dot{a}^2 + a^2 \ddot{a}}{r} \right) = \frac{p(\infty)}{\rho_o} , \tag{7.4}$$

which equation applies everywhere outside the surface of the sphere. On the surface, $r = a$ and Eq. 7.4 reduces to

$$a\ddot{a} + \frac{3}{2} \dot{a}^2 = \frac{1}{2a^2 \dot{a}} \frac{d}{dt} (a^3 \dot{a}^2) = \frac{p(a) - p(\infty)}{\rho_o} = \frac{P}{\rho_o} , \tag{7.5}$$

where $p(a)$ is the pressure in the liquid just outside the surface.

Rayleigh (1917) assumed that the pressure term is constant during bubble growth or collapse. Integrating Eq. 7.5 he found

$$a^3 \dot{a}^2 = \int_0^t 2 \frac{P}{\rho_o} a^2 \dot{a} \, dt = \frac{2}{3} \frac{P}{\rho_o} \int_0^t \frac{d}{dt} a^3 \, dt = \frac{2}{3} \frac{P}{\rho_o} \left(a^3(t) - a^3(0) \right) , \tag{7.6}$$

from which the velocity is

$$\dot{a} = \pm \sqrt{\frac{2}{3} \frac{P}{\rho_o} \left| 1 - \left(\frac{a(0)}{a} \right)^3 \right|} \tag{7.7}$$

and the acceleration is

$$\ddot{a} = \pm \frac{a^3(0) P}{a^4 \rho_o} . \tag{7.8}$$

As previously indicated, these equations can be used to predict all but the initial and final stages of bubble growth and collapse.

Except when the bubble is very small, Eq. 7.7 predicts a constant rate of growth and Eq. 7.8 confirms that the acceleration becomes very small. From Eq. 7.7 the velocity during most of the growth stage is

$$\dot{a} \doteq \sqrt{\frac{2}{3}\frac{P}{\rho_o}} . \tag{7.9}$$

Under constant tension, the bubble will grow to a maximum size given approximately by

$$a_o \doteq \sqrt{\frac{2}{3}\frac{P}{\rho_o}}\, T_g , \tag{7.10}$$

where T_g is the time spent in a negative pressure region. This result is only approximate, since it does not take into account either the acceleration and deceleration periods at the beginning and end of the expansion or the fact that the tension, P, is not always constant.

For the collapse phase, Lord Rayleigh found the total time of collapse, T_c, to be

$$T_c = \sqrt{\frac{3}{2}\frac{\rho_o}{P}} \int_0^{a_o} \frac{a^{3/2}\,da}{(a_o^3 - a^3)^{1/2}} = 0.915 a_o \sqrt{\frac{\rho_o}{P}} , \tag{7.11}$$

showing that the time of complete collapse is proportional to the *maximum bubble radius*, a_o, which, by Eq. 7.10, is itself proportional to the time of growth. Moreover, combining Eqs. 7.10 and 7.11, it is found that for the same static pressure difference the time a bubble takes to collapse is very close to three-quarters of the time it takes to grow.

In his original derivation of Eq. 7.7 for the bubble wall velocity during collapse, Rayleigh equated the sum of the kinetic and potential energies of the motion to the potential energy existing when the bubble is at its maximum radius. The potential energy at any instant is

$$E_{Pot} = PV(t) \doteq \frac{4}{3}\pi a^3 P , \tag{7.12}$$

while the kinetic energy for the entire velocity field given by Eq. 7.2 is

$$E_{Kin} = \frac{1}{2}\rho_o \int_a^\infty u^2 4\pi r^2\,dr = 2\pi\rho_o \int_a^\infty \dot{a}\left(\frac{a^4}{r^4}\right) r^2\,dr = 2\pi\rho_o \dot{a}^2 a^3 . \tag{7.13}$$

From this it follows that

$$\frac{4}{3}\pi a^3 P + 2\pi\rho_o \dot{a}^2 a^3 = \frac{4}{3}\pi a_o^3 P . \tag{7.14}$$

The velocity is given by

$$\dot{a}^2 = \frac{2}{3}\frac{P}{\rho_o}\left(\frac{a_o^3}{a^3} - 1\right) , \qquad (7.15)$$

in agreement with Eq. 7.7.

Figure 7.2 shows a typical bubble growth and collapse cycle as predicted by classical theory. Rayleigh himself recognized that compressibility must affect the final collapse stage, since

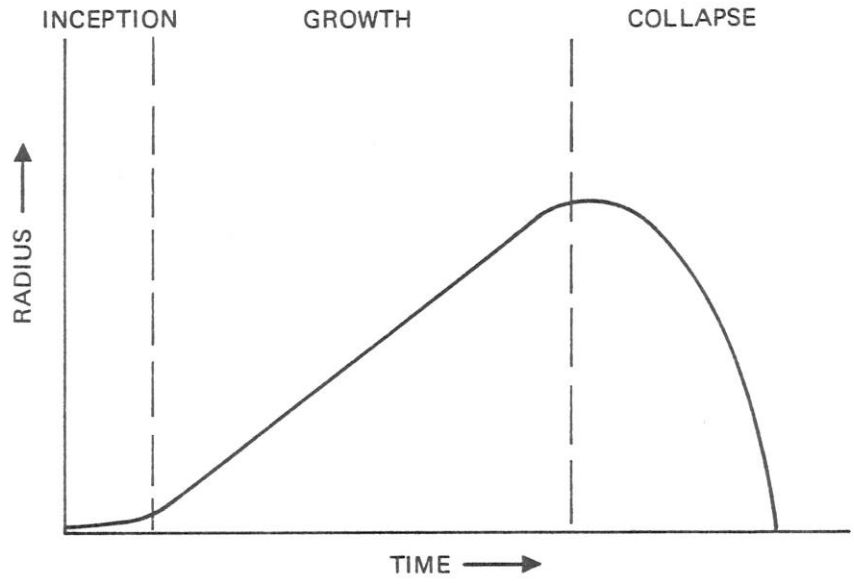

Fig. 7.2. Growth and Collapse of an Empty Bubble in an Ideal Incompressible Liquid according to Classical Theory

Eq. 7.15 predicts infinite velocity as the radius approaches zero. He also noted that, if the bubble contained any permanent gas, the kinetic energy would be consumed in compressing the gas and the motion would stop prior to complete collapse. Since his theory neglects all dissipative mechanisms, it implies that the bubble will oscillate indefinitely between its minimum and maximum radii. Such rebounding is actually observed but it dies rather quickly since energy is lost by sound radiation and heat conduction.

Photographic observations of bubble collapse reported by Knapp et al (1970) show good agreement with classical theory, except that the time of collapse is about 10% greater than that predicted.

Pressure Inside a Bubble

Rayleigh's theory deals with the pressure just outside the bubble wall, which was taken to be equal to that inside the empty cavity, i.e., to be essentially zero. Actually, as indicated by Eq. 7.1, surface tension causes the pressure inside to be greater than that outside a static bubble. Also, the bubble is not empty; it contains vapor and some permanent gas. Thus, the pressure inside a static cavity is given by

$$p_i = p_v + p_g = p(a) + \frac{2\sigma}{a} , \qquad (7.16)$$

where the surface tension is a function of temperature but is assumed to be independent of bubble radius. The gas pressure, p_g, will vary during any rapid changes of bubble volume. Since permanent gases go into and out of solution very slowly, the total amount of such gas is essentially constant, and the instantaneous gas pressure is related to an equilibrium value by

$$p_g(t) = p_{g_e}\left(\frac{a_e}{a}\right)^b , \tag{7.17}$$

where b is 3 if the process is isothermal and 3γ if it is adiabatic.

In addition to the static pressure drop due to surface tension, a moving boundary also experiences a pressure difference attributable to the viscosity of the liquid. Viscosity appears in the Navier-Stokes equations in two terms, but Poritsky (1952) has pointed out that its dominant contribution to the problem under consideration here is at the boundary between the bubble and the fluid. If the bubble is expanding, viscosity adds a single term and Eq. 7.16 becomes

$$p_i = p_v + p_{g_e}\left(\frac{a_e}{a}\right)^b = p(a) + \frac{2\sigma}{a} + 4\mu\frac{\dot{a}}{a} . \tag{7.18}$$

Bahl and Ray (1972) have shown that the surface-tension term is only significant during collapse if a_o is less than $15\sigma/p_o$. Poritsky noted that in a highly viscous liquid the viscosity term could prevent bubble collapse. However, it plays only a minor role in water.

Effects of Compressibility

As already noted, classical theory predicts infinite collapse speed as the bubble radius approaches zero. However, one would expect compressibility effects to reduce the velocity when the speed approaches a Mach number of one. Gilmore (1952) and Hunter (1960) adapted equations originally derived to treat explosion bubbles and found that compressibility effects begin to become important when the Mach number exceeds 0.3, at a relative radius of about 5%. At a relative radius of 1%, the collapse speed is calculated to be only about 40% of that predicted by classical theory.

Gilmore's analysis ignored the contents of the bubble. Actually, as will be discussed in the following paragraphs, permanent gases also tend to cushion the collapse and to limit the maximum bubble collapse speed. Compressibility only becomes important if the partial pressure of the permanent gas is less than 1% of the ambient pressure, a condition which is quite rare.

While the hydrodynamic effects of compressibility are less important than was thought during the 1950's, it is this property of the liquid that makes possible the radiation of a significant fraction of the bubble energy as sound. The radiation of sound associated with bubble collapse will be discussed in Section 7.4.

Effects of Permanent Gases

In Section 7.2 it was pointed out that permanent, dissolved gases can play a major role in determining the tensile strength of a liquid because they control the cavitation inception process. Another major effect is that of cushioning the final collapse process and storing some of the kinetic energy of a rapidly collapsing bubble as potential energy. As a result of this stored energy, bubbles do not collapse to zero radius but instead stop collapsing with a minimum radius that may be from 2 to 10% of their maximum radius. They then rebound, form new cavities and collapse

again, often repeating the process four or five times. Instead of the ideal single collapse shown in Fig. 7.2, the history is more often as shown in Fig. 7.3.

As mentioned earlier, Rayleigh (1917) recognized the importance of permanent gas in arresting the collapse motion. He assumed isothermal conditions, for which the work of compression is given by the product of the initial pressure and volume and the logarithm of the initial volume divided by the instantaneous volume. Subtracting this energy from the kinetic energy, he found

$$\dot{a}^2 = \frac{2}{3}\frac{P}{\rho_o}\left(\frac{a_o^3}{a^3} - 1\right) - \frac{2}{3}\frac{Q}{\rho_o}\left(\frac{a_o}{a}\right)^3 ln\left(\frac{a_o}{a}\right)^3 , \qquad (7.19)$$

where Q is the pressure of the permanent gas when the bubble is at its maximum radius and P is the collapse pressure.

From Eq. 7.19, Rayleigh estimated the minimum radius by setting $\dot{a}$ equal to zero, finding

$$a_m \doteq a_o\, e^{-P/3Q} . \qquad (7.20)$$

He found the maximum pressure to be

$$p_{max} = Q\left(\frac{a_o}{a_m}\right)^3 = P\left(\frac{Q}{P}\right) e^{P/Q} , \qquad (7.21)$$

from which, theoretically, the peak gas pressure becomes quite astronomical if the partial gas pressure, Q, is less than 2% of the collapse pressure, P.

It is closer to physical reality to assume that the compression of the gas is adiabatic. Noltingk and Neppiras (1950) derived an equation for a partially gas-filled bubble in an ideal, inviscid, incompressible liquid. Essentially, they modified Eq. 7.5 by a permanent gas term,

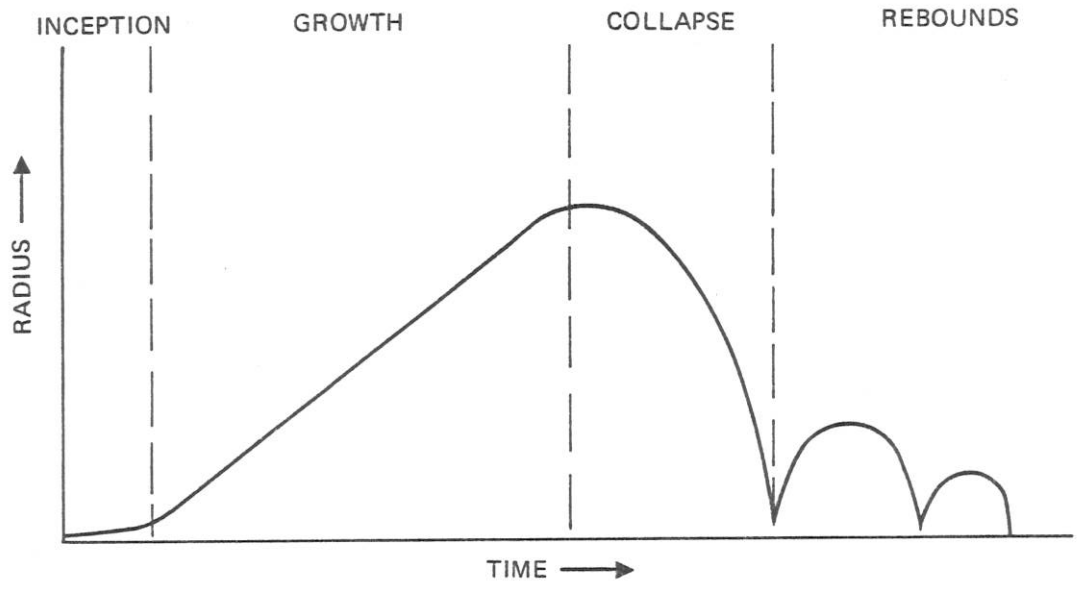

Fig. 7.3. Growth and Collapse of a Cavitation Bubble Having Finite Gas Content

$$a\ddot{a} + \frac{3}{2}\dot{a}^2 = \frac{1}{2a^2\dot{a}}\frac{d}{dt}(a^3\dot{a}^2) = \frac{P}{\rho_o}\left(1 + \frac{Q}{P}\left(\frac{a_o}{a}\right)^{3\gamma}\right), \tag{7.22}$$

from which they found the velocity to be

$$\dot{a} = \frac{2}{3}\frac{P}{\rho_o}\left(\frac{a_o}{a}\right)^3\left[1 - \left(\frac{a}{a_o}\right)^3 + \frac{Q}{P(\gamma - 1)}\left(1 - \frac{1}{\gamma - 1}\left(\frac{a_o}{a}\right)^{3(\gamma - 1)}\right)\right], \tag{7.23}$$

and the acceleration to be

$$\ddot{a} = -\frac{P}{\rho_o}\frac{a_o^3}{a^4}\left[1 + \frac{Q}{P(\gamma - 1)} - \frac{Q\gamma}{P(\gamma - 1)}\left(\frac{a_o}{a}\right)^{3(\gamma - 1)}\right]. \tag{7.24}$$

Setting the velocity equal to zero, they found the minimum radius to be given by

$$a_m \doteq a_o\left(\frac{Q}{P(\gamma - 1)}\right)^{1/3(\gamma - 1)}\left(1 + \frac{Q}{P(\gamma - 1)}\right)^{-1/3(\gamma - 1)}, \tag{7.25}$$

provided $a_m < 1/3\, a_o$. Figure 7.4 is a plot of this equation for two values of γ. The gas pressure inside the bubble corresponding to the minimum radius is

$$p_{max} \doteq Q\left(\frac{P(\gamma - 1)}{Q}\right)^{\gamma/(\gamma - 1)}\left(1 + \frac{Q}{P(\gamma - 1)}\right)^{\gamma/(\gamma - 1)}. \tag{7.26}$$

Setting $\ddot{a} = 0$, Eq. 7.24 predicts that the bubble wall will have its maximum collapse speed when

$$a_c = a_o\left(\frac{Q\gamma}{P(\gamma - 1)}\right)^{1/3(\gamma - 1)}\left(1 + \frac{Q}{P(\gamma - 1)}\right)^{-1/3(\gamma - 1)} = a_m\gamma\frac{1}{3(\gamma - 1)}, \tag{7.27}$$

and that this maximum speed will be

$$\dot{a}_{max}^2 \doteq \frac{2P(\gamma - 1)}{3\rho_o\gamma}\left(\frac{P(\gamma - 1)}{Q\gamma}\right)^{1/(\gamma - 1)}\left(1 + \frac{Q\gamma}{P(\gamma - 1)}\right)^{\gamma/(\gamma - 1)}. \tag{7.28}$$

Since the compression is assumed to be adiabatic, this theory also yields

$$\theta_{max} = \theta_o\frac{p_{max}}{Q}\left(\frac{a_m}{a_o}\right)^3 = \theta_o\left(\frac{P(\gamma - 1)}{Q}\right)\left(1 + \frac{Q}{P(\gamma - 1)}\right) \tag{7.29}$$

as maximum temperature, where both θ's are measured in degrees Kelvin. Thus, incompressible theory predicts maximum temperatures in excess of a thousand degrees provided $Q < 0.1P$.

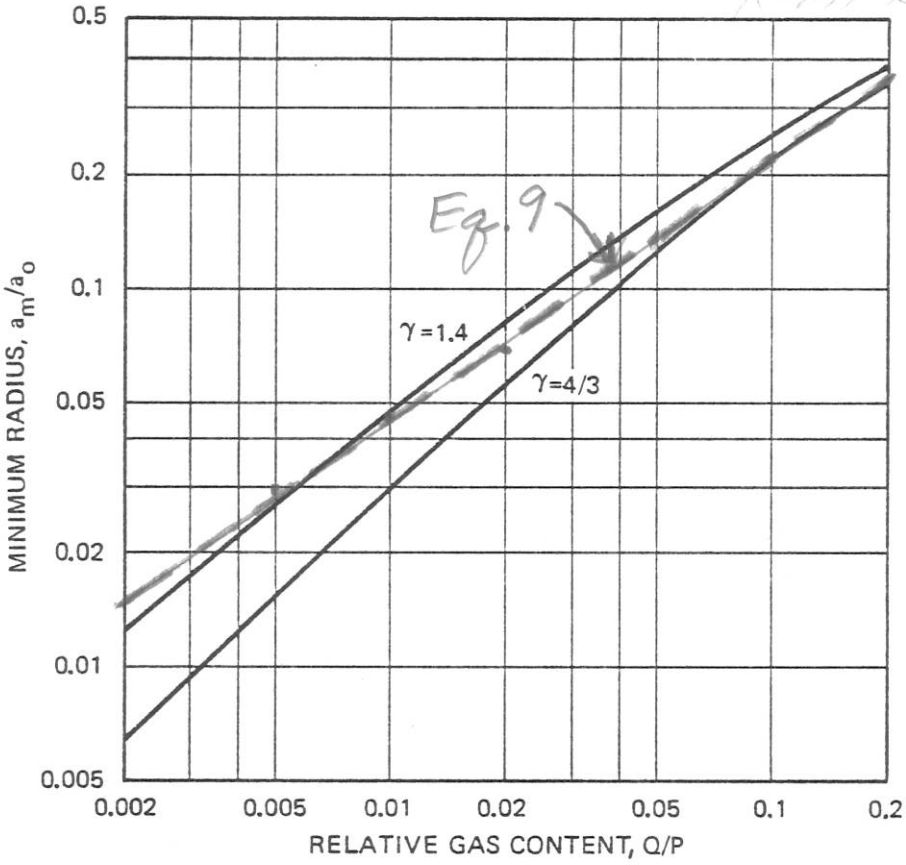

Fig. 7.4. Minimum Bubble Radius as Function of Relative Gas Content, for Two Specific Heats (Eq. 7.25)

The Noltingk-Neppiras incompressible equation can be expected to overestimate collapse speeds when it predicts Mach numbers in excess of 0.3. From Eq. 7.28, the maximum Mach number for bubble collapse is given by

$$M_{max} \doteq \sqrt{\frac{2P}{3\rho_o c_o^2}\left(\frac{\gamma - 1}{\gamma}\right)}\left(\frac{P(\gamma - 1)}{Q\gamma}\right)^{1/2(\gamma - 1)} \left(1 + \frac{Q\gamma}{P(\gamma - 1)}\right)^{\gamma/2(\gamma - 1)} \quad (7.30)$$

This can also be expressed in terms of the ratio of a_m to a_o by using Eq. 7.25 and neglecting several small terms. When this is done, the maximum Mach number is found to be virtually independent of γ for a_m/a_o up to about 0.25, corresponding to a relative gas pressure of about 10%. Over this range the maximum Mach number can be approximated by

$$M_{max} \doteq \left(0.015\,\frac{a_o}{a_m}\right)^{3/2}\sqrt{P_A} \quad , \quad (7.31)$$

where P_A is static pressure in atmospheres.

The maximum Mach number computed by the incompressible theory is plotted as a function of P/Q in Fig. 7.5. It is clear that the validity of the incompressible assumption is a function of the collapse pressure as well as the relative gas content. Thus, incompressible theory is seen to be valid for values of Q/P as low as 1% when the collapse pressure is 1 atm., but only for $Q/P > 4\%$ for a collapse pressure of 10 atm. For most practical cavitation problems, it seems reasonable to assume that the incompressible theory is valid unless the gas content is very low.

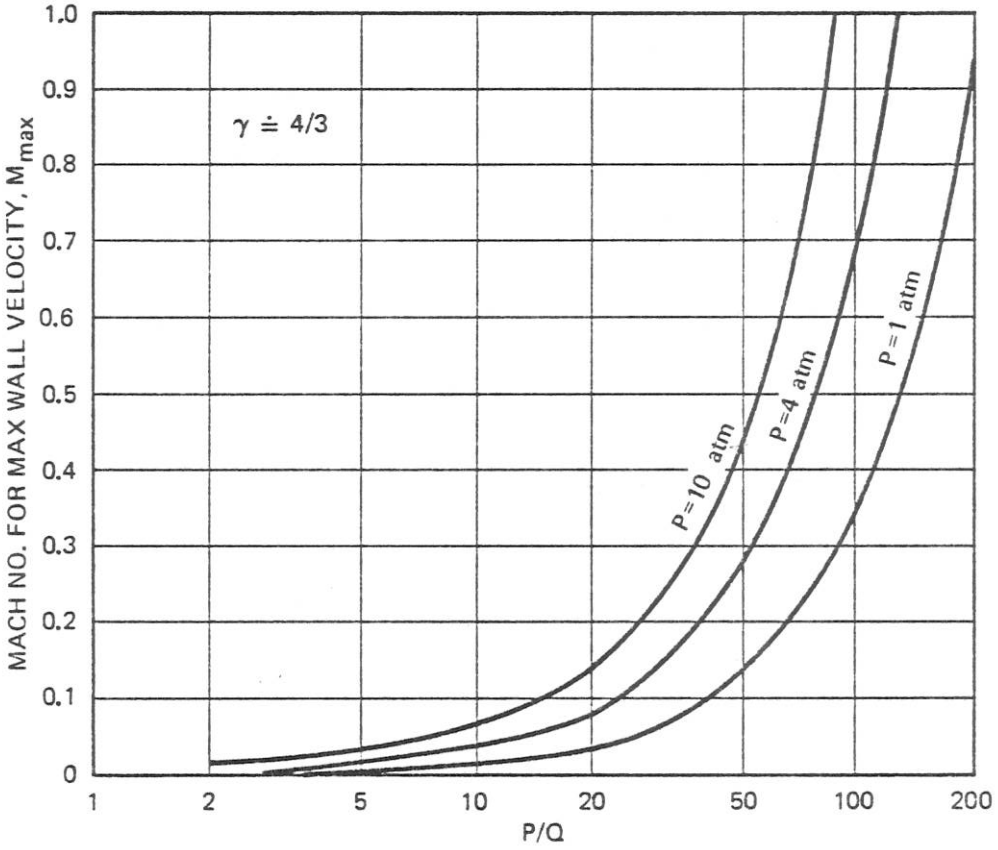

Fig. 7.5. Maximum Collapse Mach Number as a Function of Gas Content Using Incompressible Theory (Eq. 7.30)

Trilling (1952) included compressibility in his calculation of the collapse of a bubble containing gas. He assumed the speed of propagation of all disturbances to be equal to the speed of sound. Hickling and Plesset (1964) used Gilmore's (1952) results to solve for bubble motion when gas cushions the collapse. They found the minimum radius for a given gas to depend primarily on the ratio of the equilibrium gas pressure, Q, to the collapse pressure, P, and secondarily on the actual value of P. Their results for collapse pressures of 1 and 10 atm. are compared to the Noltingk-Neppiras incompressible theory in Table 7.1. Compressibility effects are seen to increase the minimum radius and thereby decrease maximum pressures and temperatures appreciably. The incompressible theory gives reasonable results if the permanent gas pressure exceeds 1% of the collapse pressure.

Within the range of validity of the Noltingk-Neppiras theory, Eq. 7.31 leads to simplification of some of the equations for bubble velocity and acceleration. Thus, Eq. 7.28 for the maximum

Table 7.1.
Comparison of Compresible and Incompressible
Theories for Collapse of Gas-Filled Cavities ($\gamma = 1.4$)

Q/P	Incompressible Theory Eq. 7.25	Compressible Theory* P = 1 bar	Compressible Theory* P = 10 bars
	Relative Minimum Radius		
0.10	0.262	0.28	
0.010	0.047	0.060	0.074
0.0010	0.0069	0.018	0.025
10^{-4}	0.0010	0.006	0.009
10^{-5}			0.0035

*After Hickling and Plesset (1964).

velocity can be replaced by

$$\dot{a}^2_{max} \doteq \frac{1}{12}\frac{P}{\rho_o}\left(\frac{a_o}{a_m}\right)^3 \qquad \left(\frac{Q}{P} < 0.1\right) , \tag{7.32}$$

and to a close approximation the wall velocity is

$$\dot{a}^2 \doteq 8\dot{a}^2_{max}\left(\frac{a_m}{a}\right)^3\left[1 - \left(\frac{a_m}{a}\right)^{3(\gamma-1)} - \left(\frac{a}{a_o}\right)^3\right] , \tag{7.33}$$

and the acceleration is

$$a\ddot{a} \doteq -12\dot{a}^2_{max}\left(\frac{a_m}{a}\right)^3\left(1 - \gamma\left(\frac{a_m}{a}\right)^{3(\gamma-1)}\right)\left(1 + \left(\frac{a_m}{a_o}\right)^{3(\gamma-1)}\right) . \tag{7.34}$$

These equations are used in the analysis of noise radiation in the following section.

The Noltingk-Neppiras equation has been used for bubble collapse analyses by Khoroshev (1963). He presented his results as a correction to classical theory, the correction factor being given as a function of the relative gas content at maximum radius, Q/P. For example, Khoroshev calculated the time of collapse from

$$T_c = \int_{a_o}^{a_m} \frac{1}{\dot{a}}\, da , \tag{7.35}$$

finding for Q/P less than about 20% that

$$T_c \doteq 0.915 a_o \sqrt{\frac{\rho_o}{P}}\left(1 + \frac{Q}{P}\right) . \tag{7.36}$$

He assumed $\gamma = 4/3$ since that value leads to tractable integrals.

Boguslavskii (1967) calculated the rate at which gas diffuses into a bubble, finding that it increases as the 5/2 power of the growth time. Since the volume grows as the cube of this time, the relative gas content diminishes somewhat as a bubble continues to grow. Gas diffusion also plays a role in the inception of acoustic cavitation and this subject has been treated in more detail by Hsieh and Plesset (1961) and by Eller (1969, 1975).

Asymmetrical Bubble Collapse

The Noltingk-Neppiras theory, like the classical theory of Rayleigh, assumes spherical growth and collapse. Early photographic studies of cavitation bubbles by Knapp et al (1948,1970) confirmed symmetrical collapse and revealed the rebound phenomenon. More recently, Ellis (1966), Ivany et al (1966), Kozyrev (1966, 1969) and Mitchell and Hammitt (1973) have all found that bubbles collapsing close to solid boundaries collapse asymmetrically. The bubbles distort into prolate spheroidal cavities and the more remote surface collapses, forming a jet which passes through the closer wall and strikes the solid boundary. It is now believed that this mechanism explains cavitation erosion, as will be discussed in Section 7.6.

Theoretical studies by Chapman and Plesset (1972), Hsieh (1972) and Plesset and Chapman (1971) confirm that a solid boundary should indeed cause toroidal collapse with the formation of a jet. However, the seriousness of this effect relative to the conclusions of the Noltingk-Neppiras theory has not been evaluated.

Summary and Conclusions

The phenomenon of bubble growth and collapse in cavitation is extremely complicated, involving motions of the liquid, compressibility, viscosity, surface tension, heat conduction, gaseous diffusion and thermodynamic effects. In addition, many bubbles collapse near a solid surface, making the assumption of spherical symmetry untenable. Despite all these complexities the dominant characteristics are correctly given by Rayleigh's classical theory for a bubble in an ideal liquid, as modified by the Noltingk-Neppiras correction to account for residual gases.

7.4 Single Bubble Cavitation Noise

Expression for Radiated Energy

The volume changes that are inherent in the cavitation phenomenon radiate sound as monopoles. Expressions were derived in Section 4.1 for the power radiated by a volume source in terms of the acoustic pressure and for acoustic pressure in terms of volume acceleration. These equations can be combined to obtain an expression for the total energy radiated in terms of the volume acceleration:

$$E_{ac} = \int_0^\infty W_{ac}\,dt = 4\pi r^2 \int_0^\infty \frac{p^2(t)}{\rho_o c_o}\,dt = \frac{\rho_o}{4\pi c_o}\int_0^t \ddot{V}^2(t)\,dt$$

$$= \frac{\rho_o}{4\pi c_o}\int_{a(0)}^{a(t)} \frac{\ddot{V}^2}{\dot{a}}\,da \,. \qquad (7.37)$$

The volume is, of course, a function of the radius, and it can readily be shown that

$$\ddot{V} = 4\pi(2a\dot{a}^2 + a^2\ddot{a}) \ , \tag{7.38}$$

from which it follows that

$$E_{ac} = \frac{4\pi\rho_o}{c_o} \int_{a(0)}^{a(t)} \frac{(2a\dot{a}^2 + a^2\ddot{a})^2}{\dot{a}}\, da \ . \tag{7.39}$$

In evaluating this integral, it is expedient to deal separately with the growth and collapse phases.

Growth Phase

For most of the growth phase, the classical result of constant wall velocity is a good approximation to actual motion. The approximate result for total radiated energy is

$$E_{ac} \doteq \frac{16\pi\rho_o}{c_o} \int_0^{a_o} a^2\dot{a}^3\, da = \frac{16\pi}{3}\left(\frac{2}{3}\right)^{3/2}\sqrt{\frac{P}{\rho_o c_o^2}}\, Pa_o^3 \ , \tag{7.40}$$

whence the ratio of radiated energy to potential energy of the bubble when fully expanded is

$$\frac{E_{ac}}{PV_o} \doteq \frac{8}{3}\sqrt{\frac{2P}{3\rho_o c_o^2}} \ , \tag{7.41}$$

which for almost all practical cases is less than 1%.

Collapse Phase

Most of the sound radiated by cavitation bubbles occurs during the collapse phase. One approach to calculating the sound radiated by a collapsing vapor-gas bubble is to use Rayleigh's classical theory to calculate volume acceleration and wall velocity and to use the Noltingk-Neppiras result for minimum radius. Using Eq. 7.15 for $\dot{a}^2$, the volume acceleration is

$$\ddot{V} = 4\pi\left[\frac{4}{3}\frac{P}{\rho_o}a\left(\frac{a_o^3}{a^3} - 1\right) - \frac{P}{\rho_o}\frac{a_o^3}{a^2}\right] = \frac{P}{\rho_o}\frac{V_o}{a^2}\left(1 - 4\left(\frac{a}{a_o}\right)^3\right) \ , \tag{7.42}$$

from which $\ddot{V}$ can also be expressed by

$$\ddot{V} = -2\pi\sqrt{\frac{2P}{3\rho_o}}\left(\frac{a_o}{a}\right)^{3/2}\frac{\left(1 - 4\left(\frac{a}{a_o}\right)^3\right)}{\left(1 - \left(\frac{a}{a_o}\right)^3\right)^{1/2}}\, a\dot{a} \ . \tag{7.43}$$

Using Eqs. 7.42 and 7.43 with Eq. 7.37, we find

$$\frac{E_{ac}}{PV_o} = \frac{-1}{2}\sqrt{\frac{2P}{3\rho_o c_o^2}} \int_1^{a_m/a_o} \left(\frac{a_o}{a}\right)^{5/2} \frac{\left(1 - 4\left(\frac{a}{a_o}\right)^3\right)^2}{\sqrt{1 - \left(\frac{a}{a_o}\right)^3}} \, d\left(\frac{a}{a_o}\right)$$

$$= \frac{-1}{6}\sqrt{\frac{2P}{3\rho_o c_o^2}} \int_1^{x_m} \frac{1 - 8x + 16x^2}{x\sqrt{x - x^2}} \, dx \,, \qquad (7.44)$$

where $x = (a/a_o)^3$.

These equations are derived under the assumption that the cavity is empty, but that somehow it suddenly stops collapsing at its minimum radius. When the more exact Noltingk-Neppiras equation is used, the results are modified slightly. As shown in Fig. 7.6, inclusion of gas causes the velocity term to decrease and the acceleration term to increase. Analysis shows Eq. 7.42 to be a good approximation for volume acceleration for the entire period. We are therefore justified in estimating sound radiation from classical theory using the Noltingk-Neppiras results only to calculate the minimum radius.

For values of a_m corresponding to relative gas contents of under 10%, integration of Eq. 7.44 yields

$$\frac{E_{ac}}{E_{pot}} = \frac{E_{ac}}{PV_o} \doteq \frac{1}{3}\sqrt{\frac{2P}{3\rho_o c_o^2}} \left(\frac{a_o}{a_m}\right)^{3/2} \doteq M_{max}\sqrt{\frac{8}{9}}. \qquad (7.45)$$

see Eq. 7.32

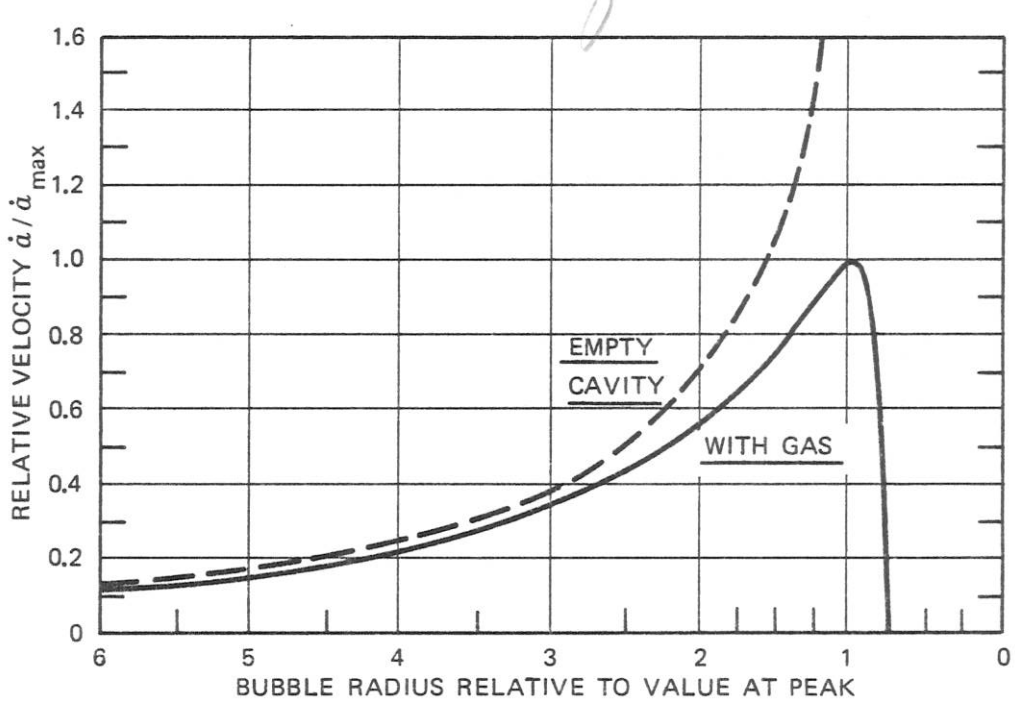

Fig. 7.6. Effect of Gas on Collapse Curve of a Bubble by Incompressible Theory (Eq. 7.33)

This simple result enables one to use previously derived expressions for the maximum Mach number to estimate the fraction of bubble energy radiated as sound. Since the Mach number is greater for lower gas concentrations and for higher collapse pressures, it follows that the fraction of potential energy radiated under these conditions is also greater.

In calculating the total energy radiated by collapse of a partially gas-filled vapor bubble, the energy for initial collapse and subsequent rebounds should be summed. Figure 7.7 shows pressure pulses corresponding to a rebound situation similar to that shown in Fig. 7.3. The total energy radiated may be assumed to be about twice that radiated during the initial collapse. It is physically impossible for a bubble to emit more sound energy than the potential energy which it had at its maximum radius; a reasonable estimate of the sound energy radiated may therefore be made by assuming that two thirds of the energy is radiated when $Q << P$ and, further, that if there is sufficient gas in the bubble to cushion the collapse and reduce the radiated sound, then double the value given by Eq. 7.45 will be applicable. Figure 7.8 uses these assumptions. It shows the fraction of potential energy estimated to be radiated as sound as a function of collapse pressure and relative gas content. When relative gas content is less than about 1/2%, it is clear that the energy radiated as sound depends entirely on the potential energy of the bubble. Relative gas contents greater than 1% should act to cushion the collapse and reduce the sound. Reductions of noise due to excess gas content were reported by Ross and McCormick (1948) and by Osborne (1947), and may also be inferred from measurements reported by others.

Acoustic Pressures

Instantaneous radiated acoustic pressure is related to volume acceleration by Eq. 3.28. From Eq. 7.42, it can be written

$$p'(t) = \frac{\rho_o \ddot{V}\left(t - \frac{r}{c}\right)}{4\pi r} = \frac{P}{3\left(\frac{r}{a_o}\right)} \left(\frac{a_o}{a}\right)^2 \left(1 - 4\left(\frac{a}{a_o}\right)^3\right) . \qquad (7.46)$$

from which the peak positive acoustic pressure is

$$p^*_{max} = \frac{P}{3} \frac{a_o}{r} \left(\frac{a_o}{a_m}\right)^2 \left(1 - 4\left(\frac{a_m}{a_o}\right)^3\right) . \qquad (7.47)$$

Assuming $\gamma \doteq 4/3$, this yields

$$p^*_{max} \doteq \frac{P}{27} \frac{a_o}{r} \left(\frac{P}{Q}\right)^2 \left[1 + 6\left(\frac{Q}{P}\right) + 9\left(\frac{Q}{P}\right)^2 - 100\left(\frac{Q}{P}\right)^3\right] . \qquad (7.48)$$

showing that, for a fixed relative gas pressure, maximum radiated pressure is proportional to the product of collapse pressure and maximum bubble radius.

As shown in Fig. 7.7, the pressure is negative during the last stage of bubble growth and the first stage of collapse. By the time the radius decreases to 60% of its maximum value, the pressure becomes positive. The negative peak, which occurs when $a = a_o$, is given by

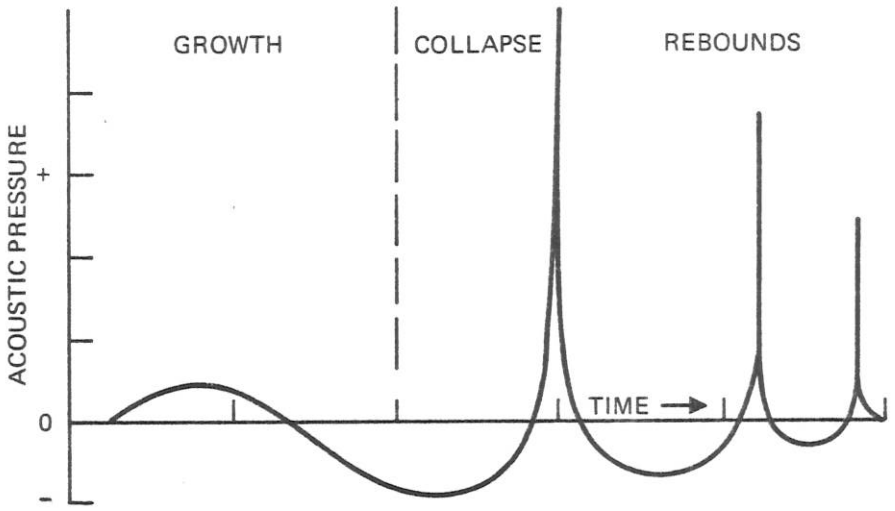

Fig. 7.7. Pressure Pulses from Collapsing Cavity

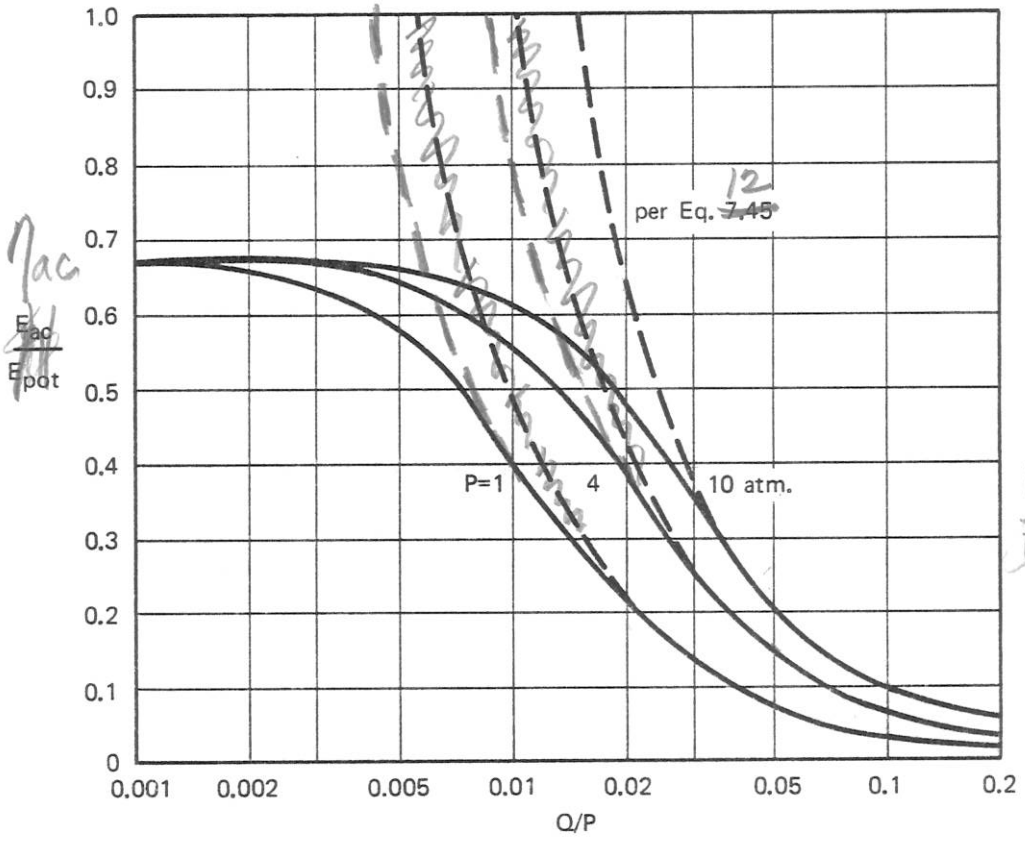

Fig. 7.8. Fraction of Energy Radiated as Sound as Function of Partial Gas Pressure

$$p^{-}_{max} = P \frac{a_o}{r} \quad . \tag{7.49}$$

The positive peak will not exceed the magnitude of the negative peak unless $Q < 0.2P$. When the partial gas pressure is less than 2% of P, the positive acoustic peak will exceed the negative one by a factor of several hundred.

Spectrum

The radiation from a collapsing bubble consists of a relatively low-frequency, negative bubble-oscillation component and a very sharp positive peak, as may be inferred from the pressure pattern shown in Fig. 7.7. The low-frequency component dominates when the gas content is high, i.e., especially for gaseous cavitation, and the positive pulse is most important for vaporous cavitation. The radiated spectrum is related to the Fourier transform of the pulse and is flat up to a high frequency equal to the reciprocal of the pulse width. Above this frequency it decreases at a rate of 6 dB/octave.

The pressure pulses emitted by collapsing bubbles having low gas content are often of sufficient amplitude to produce non-linear effects in the medium leading to shock waves. However, this does not change the conclusions drawn as to the fraction of bubble energy radiated, nor is there an important effect on observed radiated spectra.

Experimental Results

While there have been only a few experimental studies of sound radiated by collapsing cavities, the results have been similar. All of the investigators reported sharp pulses that increase in amplitude with increasing bubble size. Harrison (1952) studied single bubbles produced in the mouth of a Venturi nozzle. He found the peak pressure 10 cm from the point of collapse to be proportional to the initial collapse radius over a range from 0.2 to 1 cm. He also found that between 30 and 50% of the bubble potential energy was radiated as sound. These results are consistent with relative gas contents of about 2 to 3%. Harrison studied a spark bubble as well, getting very similar results. Mellen (1956) also studied spark-generated bubbles, finding the increase in peak pressure with bubble radius to vary as the 3/2 power to 1 cm and then linearly. His results are consistent with gas contents between 1-1/2 and 2%. The importance of gas content in controlling the radiated pulse was also confirmed by Osborne (1947).

These experiments are also in good agreement with most of the results of an analysis published by Khoroshev (1963). He also started from the Noltingk-Neppiras equation and derived expressions for acoustic pressures similar to Eq. 7.48. The analysis presented in this section has the advantage of being less complex and, in addition, it takes compressibility into account by using the fact that energy radiated as sound cannot exceed the initial potential energy of the bubble.

7.5 Broadband Cavitation Noise

Il'ichev and Lesunovskii (1963), Akulichev and Olshevskii (1968), Morozov (1968), Lyamshev (1969) and Boguslavskii et al (1970) have all treated cavitation as a random process and have used statistical methods to derive its spectral properties. Because of the pulse nature of the individual collapses and the random sequence of occurrence, the resultant spectrum covers a wide frequency range. As shown in Fig. 7.9, the spectrum rises sharply to a peak and then decreases at a rate of 6 dB/octave over a wide frequency band.

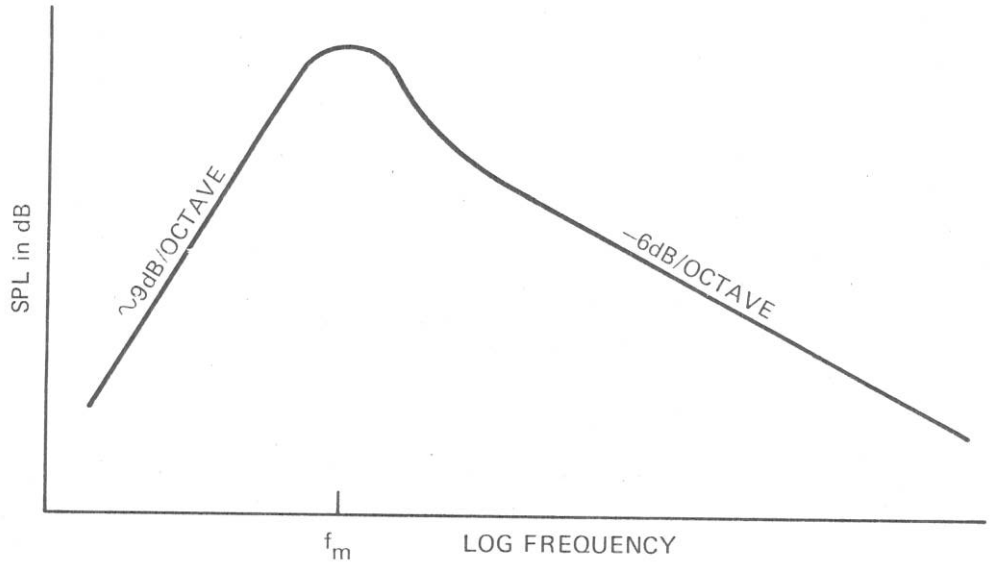

Fig. 7.9. Idealized Cavitation Spectrum

The acoustic power radiated by cavitation is the product of the average energy radiated per bubble and the number of bubbles collapsing per second. Since the energy radiated per collapse is proportional to the product of the collapse pressure and the maximum bubble volume, it follows that the radiated power is proportional to the total volume of cavitation produced per unit time,

$$W_{ac} \approx P \frac{\Delta V}{\Delta t} , \tag{7.50}$$

and that the proportionality constant is a function of the relative gas content, Q/P, as given by Fig. 7.8.

Measured cavitation spectra show peaks at frequencies related to the collapse time of the largest bubbles:

$$f_m \doteq \frac{1}{2a_o} \sqrt{\frac{P}{\rho_o}} , \tag{7.51}$$

The peak frequency is thus lower for larger bubbles. It increases, however, with collapse pressure. Below the peak, the spectrum increases at a rate of 6 to 12 dB/octave. At high frequencies, an octave or more above the peak, it decreases at a rate close to 6 dB/octave.

Several observers have noted that the intensity of high-frequency radiation decreases somewhat as cavitation becomes more developed. This may be due to increased gas content in the bubbles acting to cushion collapse and thus reduce the sound, or it may be caused by a change of acoustic properties of the medium itself due to the presence of many bubbles. Van Wijngaarden (1966) and others have noted that the sound speed is drastically reduced in a liquid containing bubbles.

Compressibility effects therefore become important at lower collapse velocities, tending to reduce maximum wall collapse speeds, Also, outer bubbles may effectively screen inner ones by absorbing energy that would otherwise radiate as sound. Akulichev and Il'ichev (1963, 1964) have pointed out that the presence of many bubbles in fully-developed cavitation may lead to additional non-linear effects, such as the production of sum and difference frequencies and the development of broad tonals at any modulation frequencies.

7.6 Other Effects of Cavitation

Only a small fraction of the vast literature on cavitation is devoted to noise aspects. Much of it is concerned with ultrasonics applications or with avoiding cavitation to prevent erosion damage. The following paragraphs give brief descriptions of some of these other phenomena associated with cavitation. Interested readers are referred to the books and articles listed at the end of the chapter.

Sonoluminescence

It has been known for over 40 years that faint light is often emitted by cavitation. Termed *sonoluminescence*, this light serves no useful purpose but must be explained by any complete theory of cavitation. There are apparently two ways in which cavitation may generate light. If the gas content of a bubble is relatively low, then compression of the small amount of permanent gas may raise its temperature above 5000°K. Thus, Eq. 7.29 predicts peak temperatures in excess of this amount if the relative gas content is less than 2%. Heat conduction, compressibility and acoustic radiation would all act to reduce the actual temperature below that calculated. Nevertheless, there is considerable experimental evidence to indicate that one source of sonoluminescence is black-body radiation of hot gas at peak compression. Thus, Kuttruff (1962) and West and Howlett (1969) have observed the timing of sonoluminescence flashes and find them to occur just ahead of or at minimum bubble volume, prior to any rebound. Jarman and Taylor (1970) confirmed this result. Spectral measurements are indicative of black-body radiation at 8,000 to 12,000°K.

On the other hand, Jarman (1959) and others have found cases of light emission when the bubble is close to its maximum radius, which they attribute to electric discharges within the bubble. Degrois and Badilian (1962, 1966, 1969) have found that sonoluminescence intensities are higher for gaseous than for varporous cavitation. They also found that hydrogen peroxide is produced by gaseous cavitation, which is consistent with electric discharges occurring inside the bubbles. It thus appears that there is a second mechanism, namely electric discharges, operative when the gas content is high, and that thermal radiation causes the sonoluminescence when the gas content is low.

Chemical Reactions

Cavitation is sometimes used to accelerate or to produce chemical reactions. Microstreaming of cavitation bubbles generates currents in liquids, a phenomenon equivalent to stirring, which thereby hastens chemical reactions. Other chemical reactions are directly caused by the high pressures and temperatures associated with cavitation or by its electric discharges. Hydrogen peroxide production and chlorine liberation from carbon tetrachloride are two examples. Depolymerization of large molecules is another example of a chemical change directly attributable to cavitation.

Erosion Damage

The longest known effect of cavitation, discovered by Parsons and others in the early days of propeller-driven steamships, is erosion damage to metals. Research in this field has taken three directions. Cavitation inception has been investigated from the point of view of developing body shapes that avoid damage by avoiding cavitation. This will be covered in sections on body and hydraulic cavitation in the present chapter. Secondly, many investigators have studied the mechanisms by which erosion takes place. The third area has been the development of materials with a high degree of resistance to cavitation erosion.

Up until about 1965, there were two competing theories of cavitation erosion: mechanical and chemical. The mechanical theory asserted that the damage was done to the eroding surface by the impingement of shock waves generated by imploding bubbles. The chemical theory postulated erosion caused by electric discharges. It is now pretty much agreed that the cause of the damage is mechanical. What occurs is fatigue failure of the metal from repeated hammer-like blows associated with cavitation bubble collapse. However, present mechanical theory differs from the older one in that it is now believed that the hammer blows are provided by impact of high-velocity liquid jets generated by asymmetrical collapse of bubbles near a solid surface. As discussed in Section 7.3, liquid jets have been observed photographically, and recent calculations indicate that they have sufficient momentum to cause the observed pitting.

Cavitation damage depends significantly on properties of the liquid, especially on its gas content. To the extent that permanent gas cushions the collapse and reduces the noise output, it also reduces mechanical forces exerted on nearby surfaces and thus reduces erosion. High temperatures of the liquid reduce damage by increasing the vapor pressure, thereby reducing collapse pressures and speeds of bubble collapse.

The literature on cavitation erosion is extensive. Some of the readily available articles are listed at the end of this chapter.

7.7 Hydrodynamically-Produced Cavitation

The two major ways that cavitation occurs in engineering systems is through the use of acoustic fields, as in ultrasonics and transducer cavitation, and by dynamic effects of liquid flows. To the student of underwater noise mechanisms the latter is of greater interest, since cavitation noise of surface ships and underwater vehicles is invariably attributable to one or more hydrodynamic cavitation sources.

The term *hydrodynamic cavitation* covers all of the ways that cavitation may occur in liquids due either to fluid flow or to movement of a body through the liquid. It is convenient to discuss hydrodynamically-produced cavitation in terms of six types distinguished from each other by the location of the cavitation. These are:

hydraulic cavitation, inside pipe systems, including Venturis, nozzles, pipe bends and valves;

body cavitation, on the surfaces of three-dimensional bodies either immersed in flows or moving through liquids;

hydrofoil cavitation, on the surfaces of two-dimensional lifting foils due to motion relative to a liquid;

vortex cavitation, in the core of a line vortex;

wake-turbulence cavitation, in the turbulent eddies of a wake, usually of a three-dimensional body; and

jet cavitation, in turbulent eddies of a jet.

These various types are discussed in this and subsequent sections of the present chapter. Their occurrence in connection with propulsors is covered in Chapter 8.

Cavitation Parameter

In treating the various types of hydrodynamic cavitation it is useful to define a dimensionless scaling parameter, K, that measures the condition of a flow relevant to cavitation. Such a *cavitation flow parameter* can be developed from consideration of the relation between static pressure, p, and flow speed, U. It follows from *Bernoulli's equation*,

$$p + \rho_o g z + \frac{1}{2}\rho_o U^2 = constant \quad , \tag{7.52}$$

that any pressure drop due to flow will be proportional to the product of density and the square of flow speed. Dividing the available static pressure, $p_o - p_v$, by the dynamic pressure of the flow leads to a dimensionless parameter, K,

$$K \equiv \frac{p_o - p_v}{\frac{1}{2}\rho_o U^2} \quad , \tag{7.53}$$

that measures the state of the flow relative to cavitation.

The cavitation parameter is reversed from most common parameters in that it actually measures the resistance of the flow to cavitation. The higher the cavitation parameter, the less likely cavitation is to occur; the lower it is, the more likely. If cavitation is occurring, lowering the flow parameter either by decreasing static pressure or by increasing flow speed will increase the extent of the cavitation; raising it may eliminate cavitation entirely.

The value of the cavitation parameter that marks the border between cavitation and no cavitation is called the *critical cavitation index*, or the *inception cavitation index*, K_i. For a given geometry it may have two values, depending on whether one starts at a point free of cavitation and measures inception, or whether one begins with existing cavitation and finds the condition for its disappearance. The former is the *incipient cavitation index* and the latter the *desinent cavitation index*. Any difference between them is referred to as *cavitation hysteresis*. These distinctions are generally not important in large engineering systems but are significant when working with models in water tunnels.

There are therefore two distinct types of cavitation parameters: a flow cavitation number, K, defined by Eq. 7.53, and, for each geometry, a critical, or inception, cavitation index, K_i. The amount of cavitation depends on the relation between these two. If the flow parameter is higher than the critical value, cavitation does not occur. Cavitation occurs only when the flow parameter is smaller than the critical value; the lower it is, the greater the extent of the cavitation zone.

Body Cavitation

The analysis of cavitation of three-dimensional bodies is an example of use of the two cavitation parameters. As shown in Fig. 7.10, whenever fluid flows past a body, the fluid must speed up near the nose. By Bernoulli's principle, there is a reduction of static pressure below the ambient value, the magnitude of the drop being proportional to the dynamic pressure of the flow velocity and dependent on the shape of the body. If the pressure drop is greater than the available static

pressure, cavitation may occur. The pressure distribution corresponding to the flow pattern of Fig. 7.10 is shown in Fig. 7.11. The flow is stopped at the nose of the body, which point is called the stagnation point. The static pressure there equals the sum of the ambient static pressure, p_o, and the dynamic pressure of the free-stream flow speed, U_o. The flow parts and speeds up and the streamlines on each side are bunched. It is in this region that body surface pressure drops below ambient, reaching a minimum value and then rising gradually. Since all pressure changes are proportional to the dynamic pressure, it is common practice to plot the pressure distribution in terms of a dimensionless pressure coefficient,

$$C_p \equiv \frac{p - p_o}{\frac{1}{2}\rho_o U_o^2}, \tag{7.54}$$

as in Fig. 7.11.

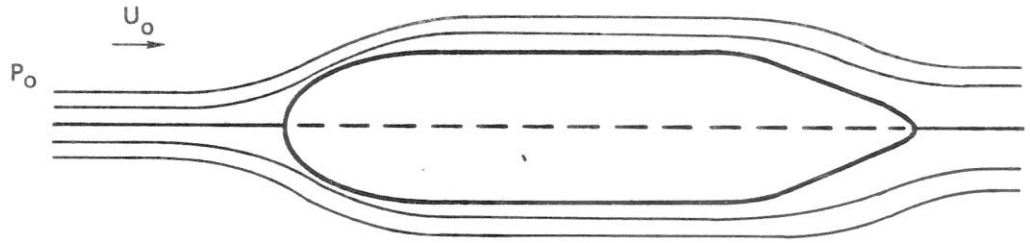

Fig. 7.10. Fluid Flow Past a Three-Dimensional Body

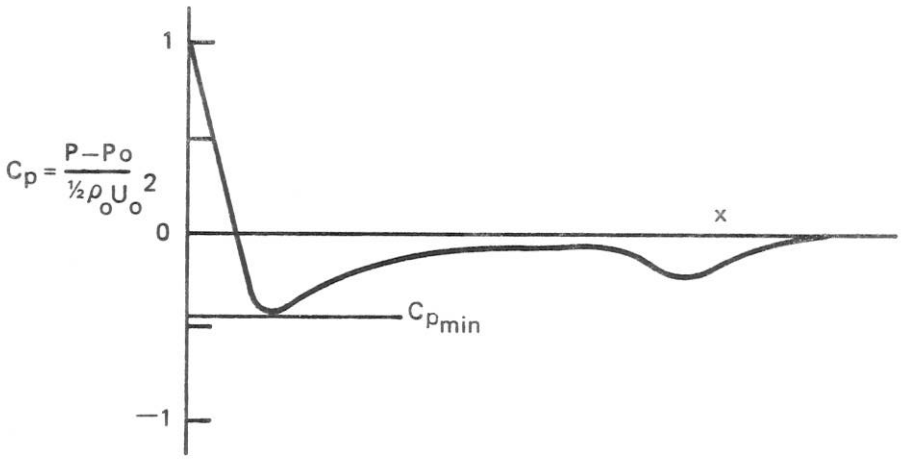

Fig. 7.11. Surface Pressure Distribution for Body in Fig. 7.10

Vapor cavitation may be expected to occur when the flow cavitation parameter is reduced to the absolute value of the minimum pressure coefficient. Thus, to a first approximation,

$$K_i \doteq \left| C_{p_{min}} \right| \quad . \tag{7.55}$$

As discussed below, cavitation inception does not always occur at the value predicted by Eq. 7.55 because of secondary, scale effects. However, for most engineering purposes, the minimum pressure coefficient is a reliable indicator of the critical cavitation index. The smaller its absolute value, the less likely cavitation is to occur.

During World War II, exhaustive studies of a variety of body shapes were carried out in several water tunnels as part of a torpedo development program. As reported by Knapp (1945), Rouse and McNown (1948) and Knapp et al (1970), critical cavitation inception indices of from 0.25 to 1.2 were found for a series of ogive noses on parallel bodies. The value for a straight body with a hemispherical nose is 0.74. Blunt semi-ellipsoidal noses have critical indices as high as 2. In general, one can expect three-dimensional bodies to have critical indices in the range 0.25 to 2. If the operational cavitation parameter is above 3, cavitation is unlikely, while cavitation is almost certain if the parameter is below 0.25.

For underwater vehicles such as submarines and torpedoes operating 10 to 15 m below the surface, body cavitation will probably not occur for speeds lower than about 10 m/sec and will be almost certain above 40 m/sec. Corresponding values for other depths are shown in Fig. 7.12, which is a plot of the cavitation parameter as a function of flow speed and depth.

While body cavitation *per se* does not appear to be a problem for most underwater vehicles, this in itself does not mean that they are free of cavitation at normal operating speeds. As will be

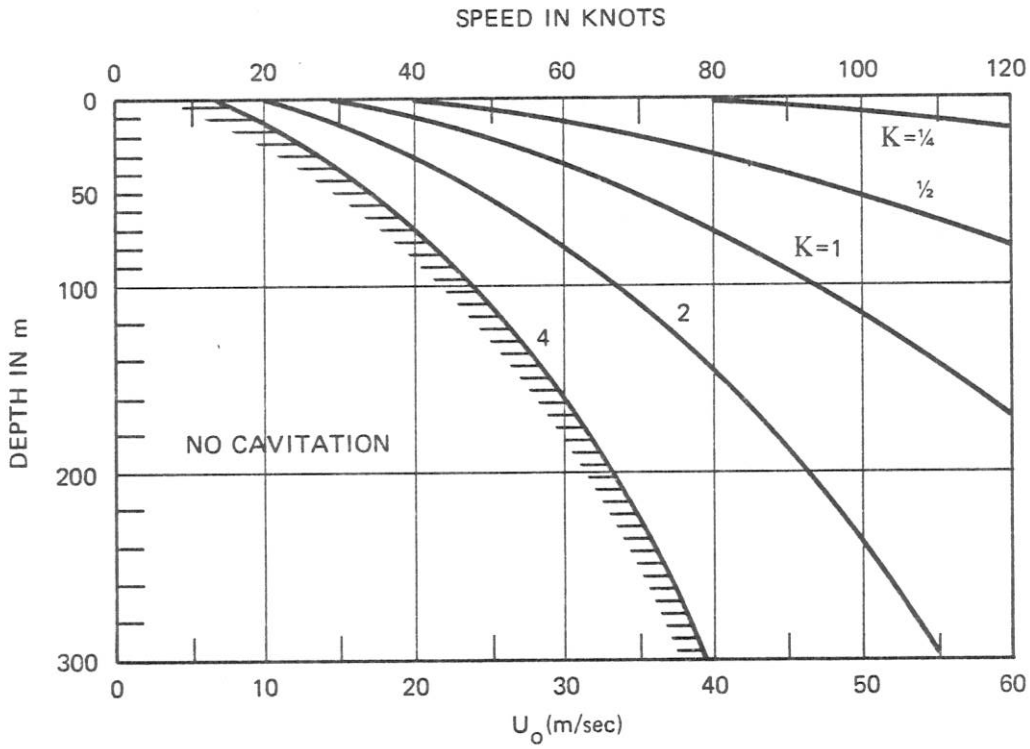

Fig. 7.12. Cavitation Parameter as Function of Depth and Speed of Advance

discussed in the next chapter, propeller cavitation occurs at much slower speeds than body cavitation. Also, any struts or fins are likely to cavitate at lower speeds than will the three-dimensional body itself.

Scale Effects

As mentioned above, the minimum pressure coefficient is often only a rough indicator of the cavitation parameter for inception. Bodies of the same shape but of different size are often found in water tunnel tests to have different values of their critical indices. In fact, even the materials used to make the test models are found to affect cavitation inception. These phenomena are all treated as scale effects.

Parkin and Holl (1953) and Kermeen et al (1955) have reported on an extensive systematic test of scale effects in cavitation inception. Tests of seven sizes of parallel bodies with hemispherical noses and of four models with ogive noses were run in two water tunnels over a speed range of 6 to 30 m/sec. Results are summarized in Fig. 7.13. In general, it was found that inception occurred for indices lower than the theoretical value, $-C_{Pmin}$. The measured inception values were closer to theoretical for larger diameter models and at the higher speeds for a given model. The data correlated with *Reynolds number*

$$R_N \equiv \frac{U_o D}{\nu} , \tag{7.56}$$

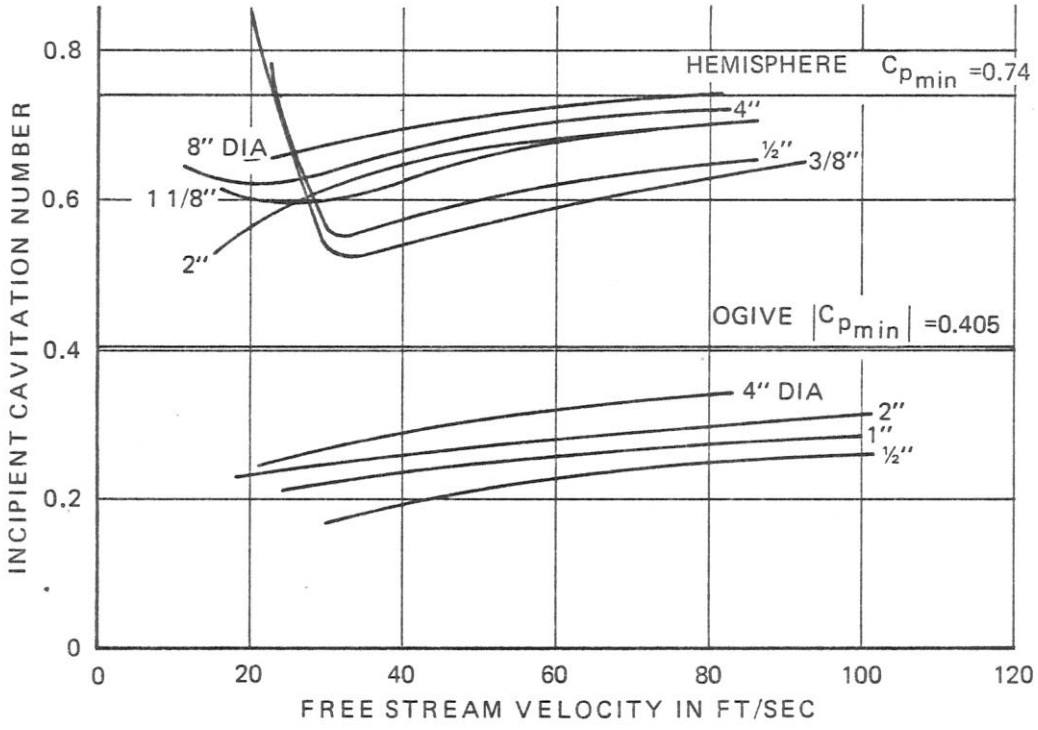

Fig. 7.13. Summary of Body Nose Cavitation Scaling Tests, as reported by Parkin and Holl (1953)

where ν is the kinematic viscosity, and with *Weber number*

$$W_N \equiv \frac{U_o \sqrt{D}}{\sqrt{\sigma/\rho_o}} \quad . \tag{7.57}$$

It was not possible to distinguish between them with any certainty.

Explanations of cavitation inception scaling in terms of nuclei dynamics have been attempted by Johnson and Hsieh (1966), Oshima (1961) and van der Walle (1962) with varying degrees of success. That scale effects are associated with nuclei growth is shown by the fact that both the nature of the model surface and the sharpness of the pressure distribution peak affect the results. Apparently nuclei can either be supplied by the model surface or by circulating microbubbles. Which of these will dominate depends on model material and on relative gas content of the tunnel water. For slow tunnel speeds and high gas contents, gaseous cavitation is often found to occur at critical indices above the theoretical value. As speed is increased and/or gas content lowered, this type disappears and vaporous cavitation occurs, at indices somewhat below theoretical. Experiments with Teflon models reported by van der Meulen (1972) seem to suggest that surface nuclei are more important than flow nuclei when inception occurs on the model surface. It would also be expected that Weber number, involving surface tension, would be more important than Reynolds number in these cases. On the other hand, Reynolds number should be more important for inception in a wake, as for sharp-edged disks, or in separated boundary layers. As reported by Holl and Wislicenus (1961), these trends have been confirmed by water tunnel tests.

Cavitation inception scaling is significant in most model testing programs and in some full-scale situations. However, it is generally not as important in practice as are the effects of roughness and of other deviations from ideal that are more commonly found in engineering systems.

Effects of Surface Roughness

Two types of deviation from smooth surface conditions have been studied in cavitation experiments. One is distributed surface roughness, produced either by applying sandpaper-like surface materials or by making grooves on the surface itself. The second is isolated, single roughness elements or protuberances. Arndt and Ippen (1968) and Arndt and Daily (1969) have treated the first case by correlating cavitation inception with the wall friction coefficient of the boundary layer. It is common practice to express the wall friction in terms of a dimensionless skin-friction coefficient, c_f, defined by

$$c_f \equiv \frac{\tau_w}{\frac{1}{2}\rho_o U^2} \quad , \tag{7.58}$$

where τ_w is the wall shear stress. Arndt and Ippen found that the smooth-wall cavitation index, K_{i_s}, is increased by a factor proportional to the skin-friction coefficient,

$$\Delta K_i \doteq 16 c_f \left(1 + K_{i_s}\right) \quad , \tag{7.59}$$

which formula is especially useful when dealing with hydraulic cavitation in rough conduits.

Isolated surface roughnesses are not so readily treated. Their effects depend upon shape, size

relative to boundary-layer thickness, and location on the parent body. Holl (1960, 1965) has correlated his results using the relation

$$\Delta K_i = K_{i_o} (1 - C_p) \quad , \tag{7.60}$$

where K_{i_o} is the incipient cavitation number for the roughness element as measured on a flat plate, and C_p is the local pressure coefficient at the location of the roughness. The flat-plate coefficient is a function of roughness shape, height relative to boundary-layer thickness, boundary-layer velocity distribution and Reynolds number. To a first approximation it is the boundary-layer velocity, u_h, at the height of the protuberance that controls the pressure drop and thereby the cavitation index. Some investigators write

$$K_{i_o} = K_h \left(\frac{u_h}{U} \right)^2 \quad , \tag{7.61}$$

where K_h depends on shape and on the Reynolds number defined in terms of u_h,

$$R_h = \frac{u_h h}{\nu} \quad . \tag{7.62}$$

Thus, Borden (1966) has found that Holl's data on isolated roughnesses correlate well with an expression of the form

$$\log K_h = - A + B \log R_h \quad , \tag{7.63}$$

where A varies from 0.14 to 0.26 for two-dimensional roughness elements and from 0.7 to 1.7 for three-dimensional ones. B is as low as 0.014 for a two-dimensional circular-arc bump, 0.10 for hemispheres and triangles and 0.37 for cylinders protruding normal to the surface.

Vortex Cavitation

Vortices associated with both lift and drag occur frequently in practical fluid flows. A *vortex* is a rotating flow; the bathtub vortex is a familiar example. Because of its rotation and the action of centrifugal force, the center of a vortex is a region of reduced static pressure where cavitation will occur if the vortex motion is strong enough. Since vortices are so common, they are often dominant sources of cavitation noise.

Although not an exact representation, most real vortices can be treated as ideal rectilinear vortices for which a central core rotates as a solid body and for which the flow outside the core obeys the laws of irrotational flow. The velocity field outside the core is often called the induced velocity field. Figure 7.14 shows an ideal vortex and the associated velocity and pressure fields. The core of radius a has an angular speed ω. Inside the vortex, the linear speed at any radius is $u = \omega r$. The strength of the vortex is measured by the maximum value of the circulation:

$$\Gamma \equiv 2\pi a u(a) = 2\pi a^2 \omega \quad . \tag{7.64}$$

The induced velocity field satisfies the relation that curl $\vec{u} = 0$, which means that the product of the linear velocity and the radial distance is constant:

$$u(r) = \frac{a}{r}\, u(a) = \frac{\Gamma}{2\pi r} \quad . \tag{7.65}$$

As derived by Dean (1944), the pressure at the vortex surface, $r = a$, relative to the pressure at infinity is given by

$$p_\infty - p_a = \frac{1}{2}\, \rho_o u^2(a) = \frac{\rho_o \Gamma^2}{8\pi^2 a^2} \quad . \tag{7.66}$$

Inside the vortex, the centripetal force relation is

$$\frac{dp}{dr} = \rho_o r \omega^2 = \rho_o r \frac{\Gamma^2}{4\pi a^4} \quad . \tag{7.67}$$

Integrating from the outer radius into the center,

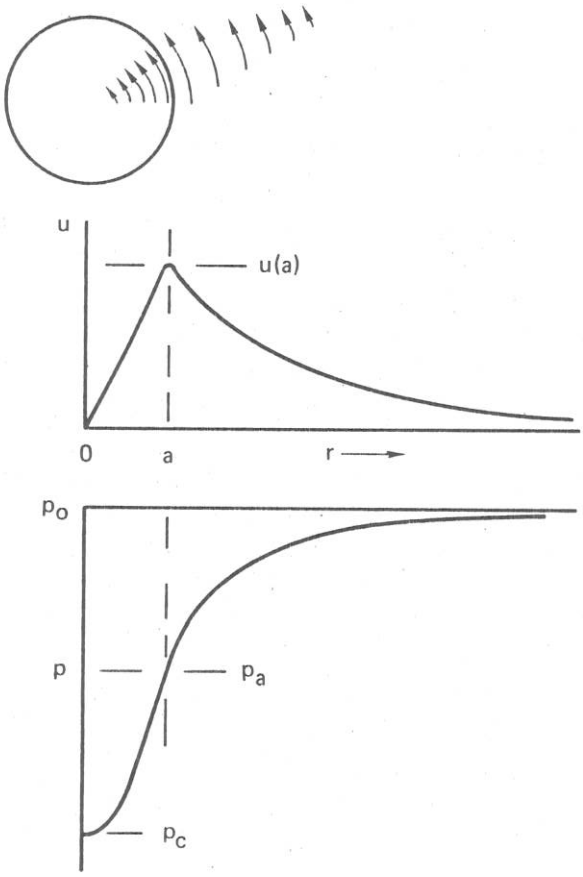

Fig. 7.14. Ideal Rectilinear Vortex

$$p_a - p_c = -\int_a^0 \frac{\rho_o \Gamma^2}{4\pi a^4} r dr = \frac{\rho_o \Gamma^2}{8\pi^2 a^2} . \tag{7.68}$$

The pressure drop inside the vortex therefore equals that outside the vortex and the total pressure drop is

$$p_\infty - p_c = \frac{\rho_o \Gamma^2}{4\pi^2 a^2} . \tag{7.69}$$

The smaller the core radius, the greater is the pressure drop associated with a given strength of vortex. If the vortex is occurring in a flow of speed U, then the incipient cavitation index of the vortex can be estimated from the pressure drop as

$$K_i \doteq \frac{p_\infty - p_c}{\frac{1}{2}\rho_o U^2} = \frac{1}{2}\left(\frac{\Gamma}{\pi a U}\right)^2 = 2\left(\frac{u(a)}{U}\right)^2 , \tag{7.70}$$

again showing the critical dependence on the core radius or, alternatively, on the maximum velocity, $u(a)$.

Vortex cavitation is quite common on propellers, as will be discussed in Chapter 8. Vortices also occur at wing tips. When airplanes fly very high, vapor may condense in wing-tip vortices which then become visible as *contrails*. In water, similar vortices cavitate. A discussion of wing-tip vortex cavitation follows that of hydrofoils at the end of Section 7.8.

Wakes and Jets

When relatively sharp-edged bodies are immersed in fluid flow, flow separation may occur at the edges and highly turbulent wakes may be produced. In such cases, as in underwater jets, cavitation first occurs at pressure minima associated with strong turbulent eddies. As for vortex cavitation, the amount of the pressure drop, and hence the value of the inception index, depends very much on Reynolds number. In fact, in a study of jet cavitation Jorgensen (1961) found a change of inception index of a factor of 3 for a Reynolds number change of about 8. Jorgensen also measured the sound radiated when the jet was thoroughly cavitating, finding the acoustic conversion efficiency to be between 0.5 and $3 \times 10^{-3} M$, where M is the jet Mach number. The measured spectra rose at the rate of 12 dB/octave to a peak and then dropped at about 6 dB/octave. Shalnev (1951) observed that cavitation in wakes exhibits a periodicity that corresponds to the shedding frequency of the strongest vortices or eddies.

7.8 Hydrofoil Cavitation

Hydrofoil, or strut, cavitation is similar to body cavitation. However, two-dimensional hydrofoils are generally more susceptible to cavitation than are three-dimensional bodies of similar thickness and cross-sectional shape. Not only does the two-dimensionality produce larger pressure changes, but also the effects of operating at angles other than head-on may be very large. Figure 7.15 shows a hydrofoil at an angle of attack to the flow together with its pressure distribution. The negative pressure region is sharper than that for the same hydrofoil at a smaller angle of

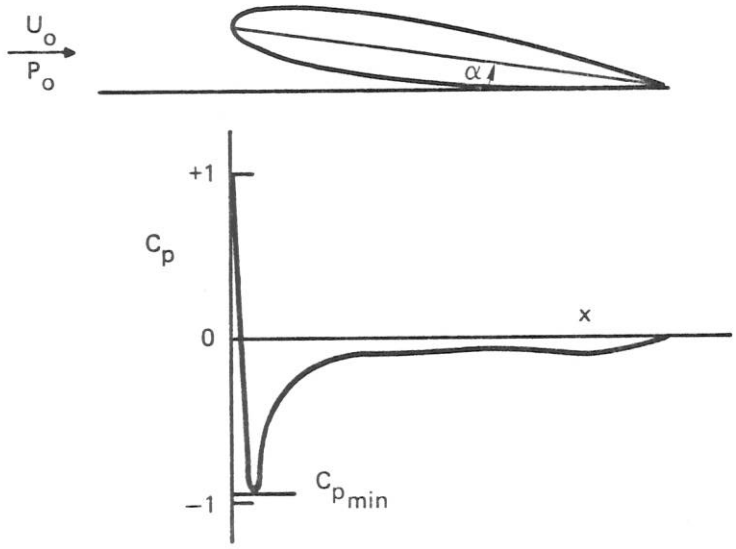

Fig. 7.15. Hydrofoil at Angle of Attack and Corresponding Pressure Distribution

attack. Critical cavitation indices of hydrofoils can be estimated from airfoil pressure distributions given in standard works on airfoils such as that of Abbott and von Doenhoff (1959). They present data on critical Mach numbers for airfoils from which minimum pressure coefficients can be obtained.

Symmetric Struts

The critical inception indices of symmetric struts at zero angle of attack are dependent primarily on thickness and secondarily on details of the profile. Figure 7.16 is a plot of the minimum pressure coefficient, assumed to equal the critical cavitation index, as a function of thickness-chord ratio for a number of symmetric hydrofoil families. To a first approximation, with a spread of ±25%,

$$K_i \doteq \left| C_{p_{min}} \right| \doteq 3 \frac{b}{s} \quad . \tag{7.71}$$

Based on this result, one would expect that the optimum strut form would be as thin as possible with a flat pressure distribution. Actually this is not always the case. If the gas content is high, flat pressure distributions having long growth times for nuclei are susceptible to gaseous cavitation. Also, as will be discussed shortly, such sections are likely to be quite sensitive to relatively small changes of the angle of attack. The optimum strut section is thus one whose design minimum pressure coefficient is only slightly lower than the minimum flow cavitation parameter for the particular application. Values of K_i of less than 0.3 are extremely difficult to achieve in most practical circumstances, and values around 0.5 are more typical.

Lifting Hydrofoils

Hydrofoils are often used to produce lift as sections of wings and of propeller blades. Lift is usually achieved by both curvature of the section, called *camber*, and by operation at a positive angle of attack. Figure 7.17 shows the contour of a typical section designed to be used as a lift-producing hydrofoil. A cambered section is generally best used at an angle of attack such that the flow is close to parallel to the camber line at the nose of the section. The angle for which this occurs is called the *design angle of attack*.

The total force experienced by a lifting foil can be resolved into two components, one perpendicular to the flow, *lift*, and one parallel to the flow, *drag*. Since both of these forces are proportional to the size of the section and to the dynamic pressure of the relative flow, it is usual to express them by dimensionless coefficients,

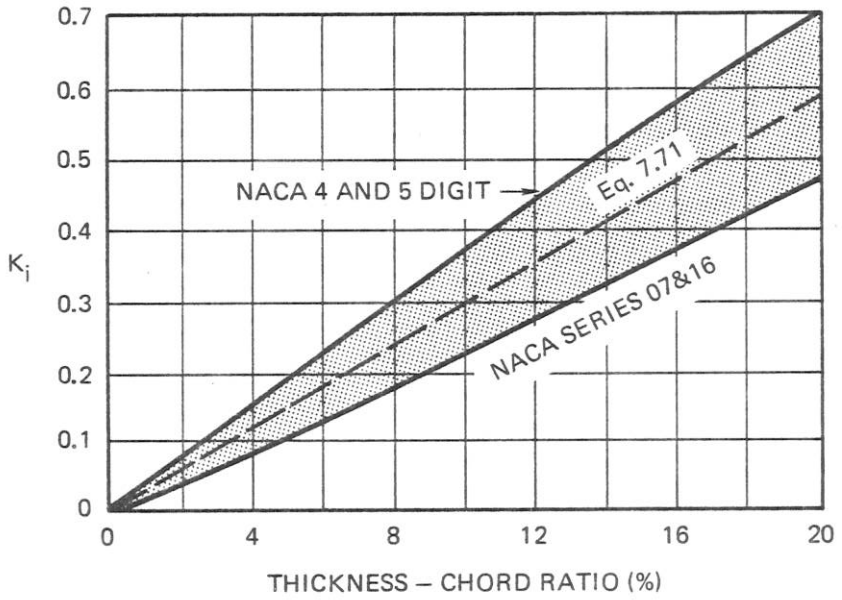

Fig. 7.16. Critical Cavitation Indices for Symmetric Hydrofoils at Zero Angle of Attack Based on Minimum Pressure Coefficients

Fig. 7.17. A Typical Lifting Hydrofoil Section

$$C_L \equiv \frac{F'_L}{\frac{1}{2}\rho_o U^2 s} \tag{7.72}$$

and

$$C_D \equiv \frac{F'_D}{\frac{1}{2}\rho_o U^2 s} , \tag{7.73}$$

where F'_L is the lift per unit width, F'_D is the drag, and s is the chord length of the section. This lift is approximately a linear function of the angle of attack over the useful range of attack angles,

$$C_L \doteq \bar{a}(\alpha - \alpha_o) , \tag{7.74}$$

where α_o is the angle producing zero lift and $\bar{a}$ is approximately 0.1/deg, or 1.8π/radian. The drag coefficient has a minimum value near the design angle of attack and increases slowly at first and then very rapidly as the angle deviates from optimum. The lift and drag coefficients for a typical airfoil, the NACA 4412 section, are shown in Fig. 7.18 as a function of angle of attack. The break in the lift curve and rapid increase in drag at an angle of 14° are caused by flow separation. Since strong wake cavitation is also associated with separation, it is a condition to be avoided. The lift coefficient at separation is termed the *maximum lift coefficient*, $C_{L_{max}}$.

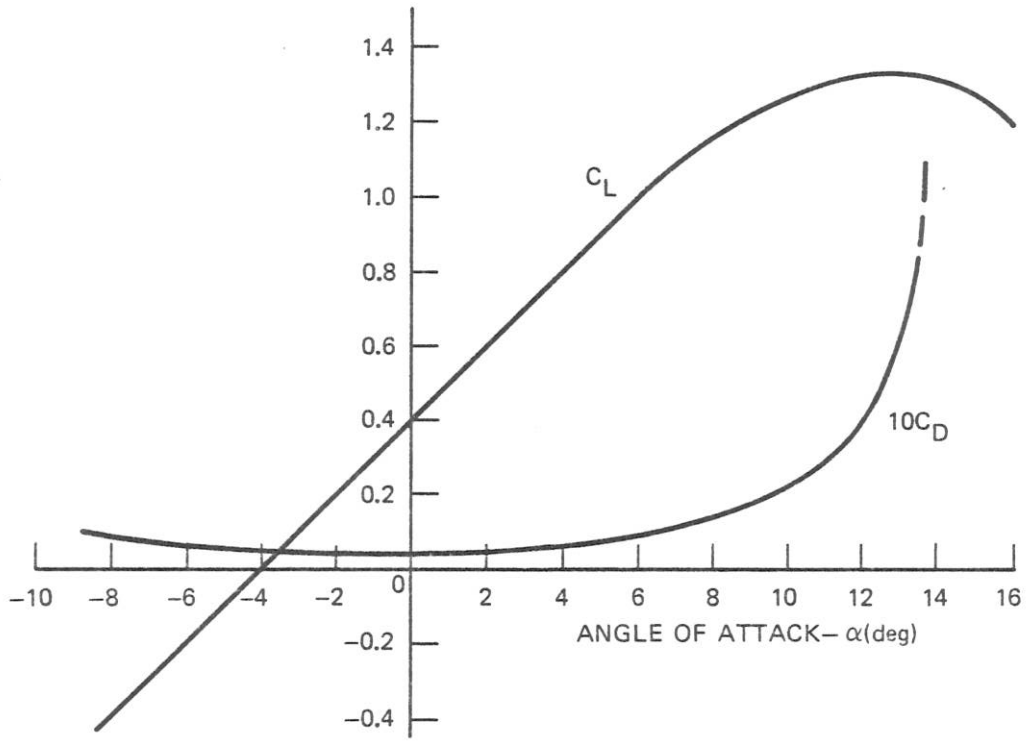

Fig. 7.18. Lift and Drag Coefficients of NACA 4412 Airfoils

Daily (1949) and Kermeen (1956) have measured the critical cavitation index of NACA 4412 hydrofoils and find good agreement with the minimum pressure coefficient as derived from data given by Abbott and von Doenhoff (1945, 1959). As shown in Fig. 7.19, the minimum pressure coefficient is smallest at or near the design angle of attack, and increases approximately parabolically as a function of angle to either side. Cavitation occurs on the suction surface at positive angles of attack and on the pressure face when the angle of attack is negative.

Airfoil sections have been developed by the N.A.C.A. (now N.A.S.A.) and other organizations in families in which a given basic shape is combined with camber functions to develop dozens of related shapes. By using different combinations of thickness, camber and angle of attack, one can produce the same lift with any member of a family. However, the minimum pressure coefficient, and consequently the critical cavitation index, will differ greatly. Ross (1947) studied several NACA airfoil families and concluded that for most families the minimum achievable cavitation index is given by

$$K_{i_{min}} \doteq K_{i_{sym}} \ (\alpha = 0) + 0.6 C_L \ . \qquad (7.75)$$

To achieve this minimum, the lift must be obtained primarily by camber and the section operated at close to its design angle of attack.

The choice of proper combinations of camber and angle of attack is very important. Thus, critical cavitation indices of hydrofoils producing a lift coefficient of 0.4 may vary from a minimum of about 0.6 to a maximum of 2.5, the highest values being found for relatively thin sections operated at angles of attack that are not optimum for the particular sections. This point is illustrated in Fig. 7.20, which shows critical cavitation indices for four symmetric sections in the same family. It is clear from this figure that relatively thin sections have lower critical cavitation

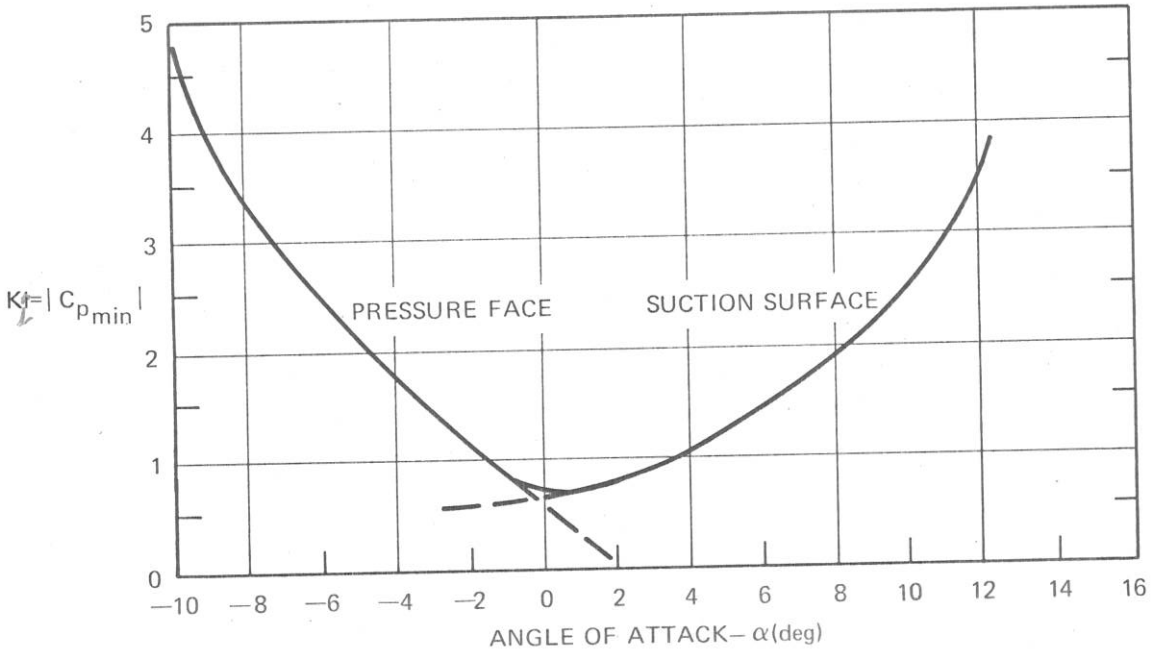

Fig. 7.19. Critical Cavitation Inception Index for NACA 4412 Hydrofoil, after Daily (1949) and Kermeen (1956)

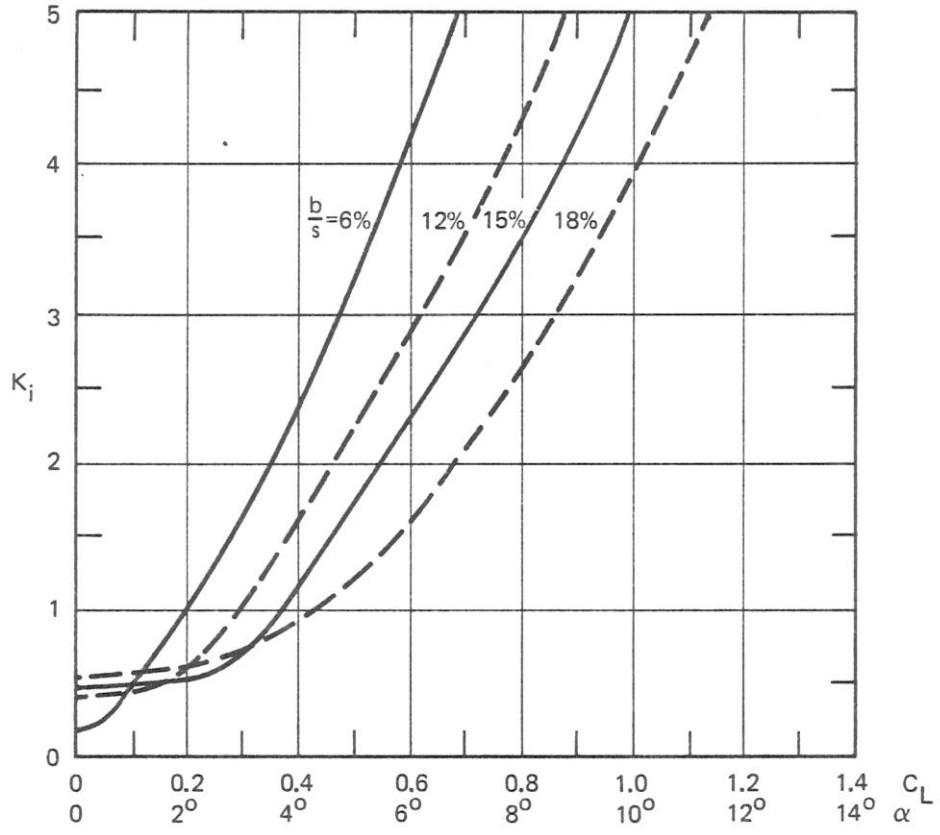

Fig. 7.20. Critical Cavitation Inception Indices Estimated for Four Symmetric NACA Series 65 Hydrofoils

indices when operated at design conditions, in accordance with Eq. 7.71, but that away from design angle thick sections are usually better.

The curves of Fig. 7.20 have important implications relevant to the choice of optimum sections in practical applications. Almost all flow situations experience fluctuations of angle of attack as well as of flow speed. Thin sections have much less tolerance for changes in attack angle than do thicker ones. As a result, a thicker section may be the better choice. In Fig. 7.20 the 6% thick section has the lowest index at zero lift, but the highest at angles greater than 1-1/2° from optimum. The 18% thick section, on the other hand, is the poorest near zero angle and is best for angles in excess of 3°.

The choice of hydrofoil sections for optimum cavitation performance is as much governed by the variability of inflow conditions as by mean values. The camber function should be chosen on the basis of mean inflow and mean lift to be produced, but the optimum thickness-chord ratio is more dependent on expected variations of inflow angle.

Effects of Cavitation on Section Performance

When a hydrofoil experiences cavitation, the pressure distribution on the cavitating surface is altered. Flow streamlines are changed in such a way that static pressure in the cavitating region is close to vapor pressure. Thus, the minimum surface pressure coefficient of a cavitating hydrofoil equals the operating cavitation parameter rather than having a larger negative value. The loss of

suction pressure reduces the lift developed. Figure 7.21 shows how the lift coefficient of a typical hydrofoil is limited by cavitation when the operating cavitation number alters the pressure distribution, and Fig. 7.22 shows how suction-surface pressure distributions are affected by cavitation.

Cavitation also affects section drag. A small amount of cavitation increases the drag but operation at a very low cavitation parameter reduces it. An alternate presentation showing the effects of cavitation is to plot C_L and C_D as functions of the operating cavitation parameter for constant angles of attack. Figure 7.23 shows lift and drag curves for the NACA 4412 section for two typical angles of attack. The peak drag is seen to occur at an operating parameter of about 40% of the critical inception value.

Scale Effects

Many hydrofoils when operated near their design angles of attack have relatively flat pressure distributions. Holl (1960) reports that they are subject to gaseous cavitation if the gas content is sufficiently high and the flow speed not too great. Otherwise, hydrofoils tend to cavitate first in the turbulent eddies of their boundary layers, the inception of cavitation depending on both flow speed and section size.

Roughness also affects hydrofoil cavitation, pretty much in the same way as for three-dimensional bodies. In fact, many of the roughness results presented in Section 7.7 are based on experiments performed on two-dimensional models and/or calculations made for two-dimensional flows.

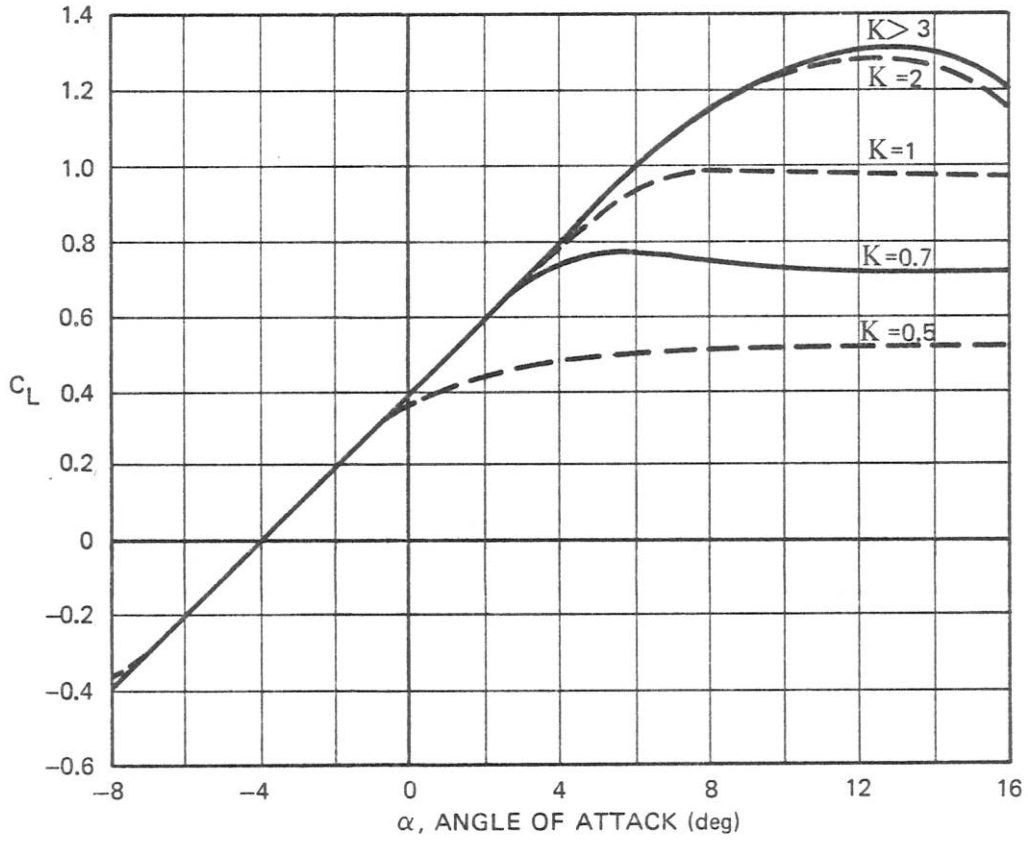

Fig. 7.21. Lift Curve for NACA 4412 Hydrofoil as a Function of Operating Cavitation Parameter, after Kermeen (1956)

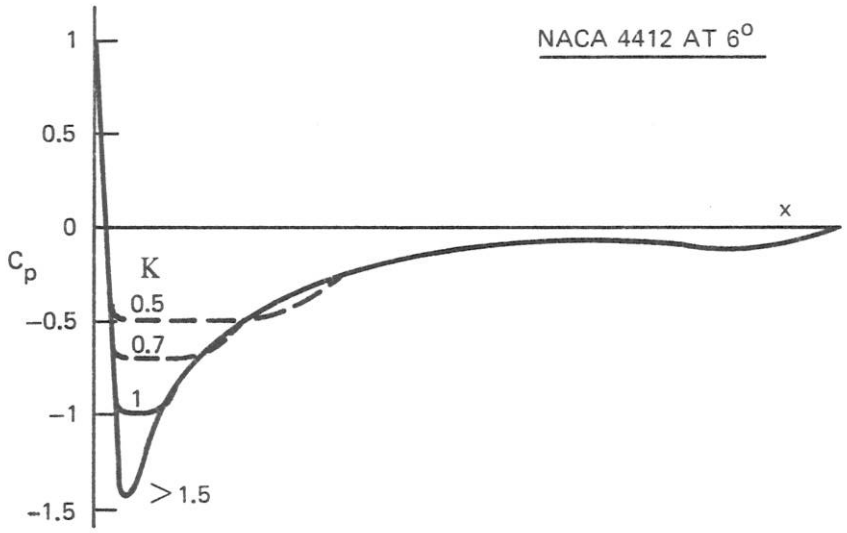

Fig. 7.22. Suction-Surface Pressure Distribution as a Function of Operating Cavitation Parameter

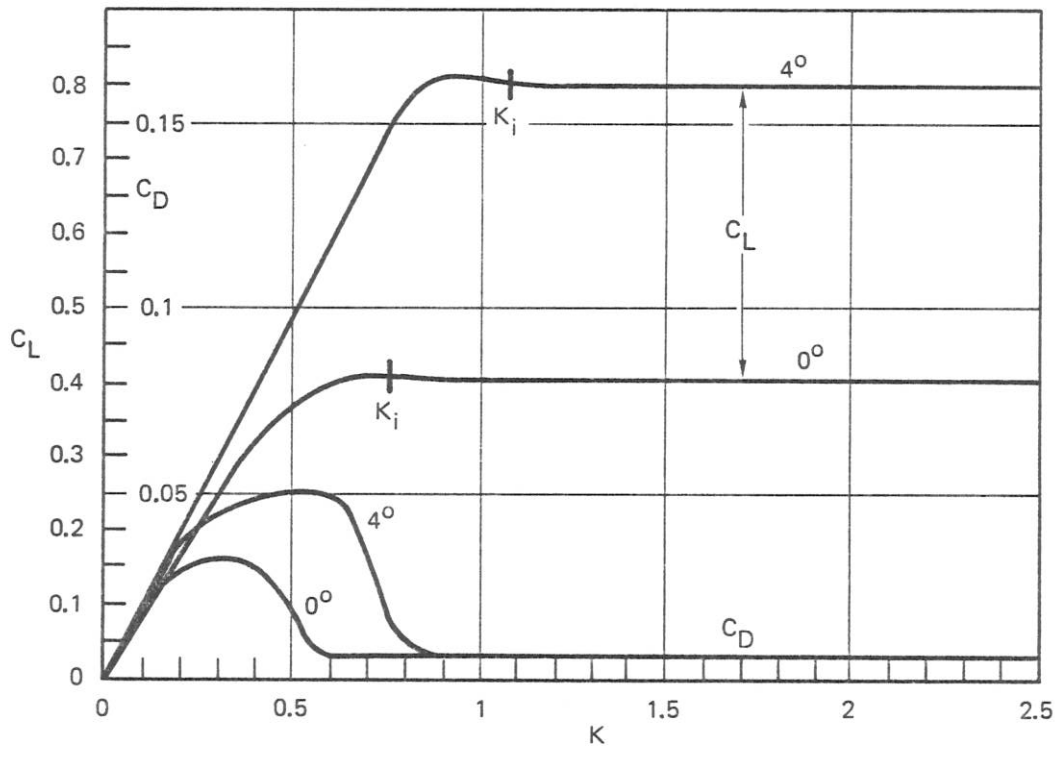

Fig. 7.23. Lift and Drag of NACA 4412 as a Function of Operating Cavitation Parameter, after Kermeen (1956)

Wing-Tip Vortex Cavitation

Hydrofoils are usually found as sections of finite wings or propeller blades. Their cavitation behavior in finite structures is modified somewhat by three-dimensional aspects of the flow. However, the most important difference is the formation of wing-tip vortices, which often cavitate at higher values of K than the sections themselves.

To understand why these vortices occur, one may either examine the flow over a wing tip in detail or consider the vortex theory of lifting surfaces. According to the vortex theory, any lifting surface may be replaced by an equivalent system of vortices having total strength equal to the circulation around the section. The lift per unit span is related to the circulation by

$$F_L' = \rho_o \Gamma U_o \ . \tag{7.76}$$

and the circulation is related to the lift coefficient by

$$\Gamma = \frac{1}{2} s C_L U_o \ . \tag{7.77}$$

Vorticity is continuous. Any spanwise change of wing section circulation results in discharge of vorticity into a vortex sheet that trails behind the wing. Since the greatest changes of circulation occur near the wing tips, the shed vorticity is strongest there. The vorticity shed at the wing tip forms a tip vortex, which will cavitate if the pressure drop is greater than ambient pressure.

Vortex cavitation has been studied by Ackeret (1930) and by McCormick (1962). Figure 7.24 shows wing-tip vortices observed by McCormick. He measured the incipient cavitation index as a function of angle of attack and attempted to correlate his results with classical wing theory.

In basic wing theory, the wing is treated as a single horseshoe vortex, and the circulation of the tip vortex equals that of the wing. Combining Eqs. 7.70 and 7.77, the cavitation index of such a horseshoe vortex would be

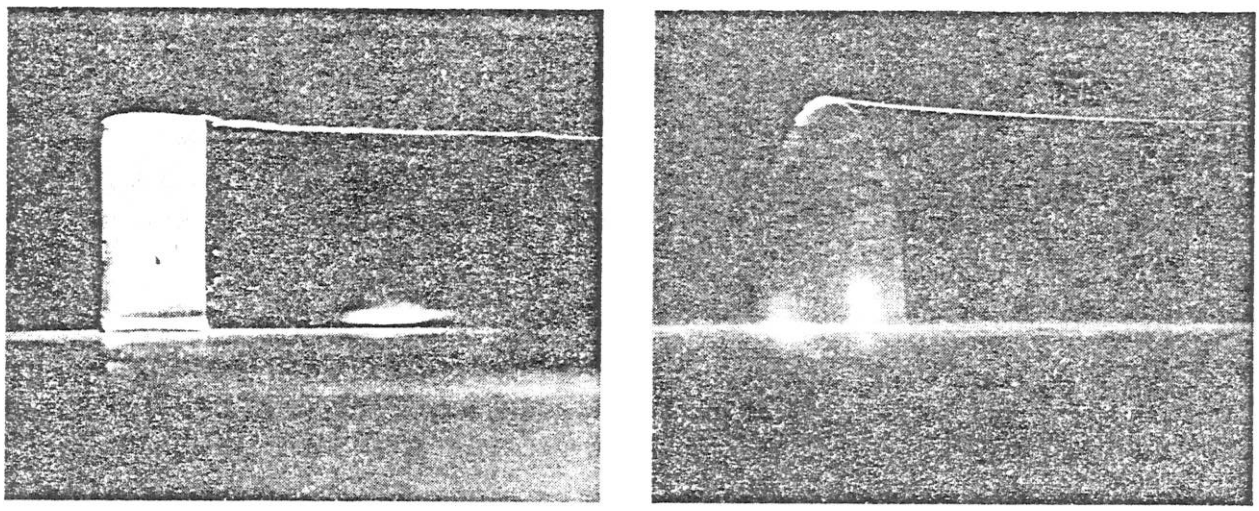

Fig. 7.24. Two Examples of Wing Tip-Vortex Cavitation, from McCormick (1962)

$$K_i \doteq \frac{1}{2}\left(\frac{\frac{1}{2}sC_L U}{\pi a U}\right)^2 = \frac{C_L^2}{8\pi^2\left(\frac{a}{s}\right)^2} , \tag{7.78}$$

showing dependence on the square of the lift coefficient and therefore of the angle of attack as well as inverse dependence on the square of the core radius relative to the section chord. McCormick confirmed that critical cavitation indices of a number of wings varied approximately as the square of the angle of attack. The problem was to calculate the core radius theoretically. Ackeret had equated the so-called induced drag associated with the tip vortices to their energy per unit length, finding $a = 0.086b$, where b is the wing span. However, McCormick found this relation to be at variance with his experimental results. One problem is that this theory leads to an expected dependence on aspect ratio, and McCormick found none. Another is that it predicts cavitation indices independent of Reynolds number, and he found a strong dependence on this factor.

In his own theoretical development McCormick related the core thickness to the thickness of the boundary layer developed on the lower surface. He concluded that the shape of the tip would be important and also that roughness of the pressure surface would affect cavitation inception. His experimental results are consistent with these theories. He predicted a strong Reynolds number effect, which was confirmed by tests over a 10:1 range, for which the inception index more than doubled. McCormick developed a rather complex equation to correlate his experimental data. However, conformity to his data within a reasonable scatter is given by

$$K_i \doteq 0.3 + 3C_L^2 , \tag{7.79}$$

where C_L is measured about one chord length from the wing tip, and the Reynolds number is about 10^6.

Supercavitating Hydrofoils

Cavitation is unavoidable for very fast surface craft. Rather than using conventional section shapes, it is preferable in such cases to use special hydrofoils which resemble wedges and which operate with fixed large cavities on the suction surface. The lift is then obtained from positive pressures on the lifting surface. Such hydrofoils designed to operate at cavitation numbers below 0.2 are called supercavitating hydrofoils. Since the cavity usually extends beyond the section, such foils are somewhat less noisy than standard hydrofoils for which individual bubbles collapse on the sections themselves.

7.9 Hydraulic Cavitation

Hydraulic cavitation generally refers to cavitation in enclosed systems such as pipes and conduits. Local pressure drops occur in such systems wherever there are constrictions or bends or where there are isolated roughnesses or other contour discontinuities. The criteria for cavitation inception are essentially the same as for hydrodynamic cavitation. A flow cavitation parameter can readily be defined for the undisturbed flow, and the critical inception index is usually about equal to the absolute value of the minimum pressure coefficient.

Pipe Constrictions

Pipe constrictions are either smooth and gradual as in a Venturi meter, or abrupt as for an orifice plate. Figure 7.25 shows the pressure drop associated with a well-designed, gradual Venturi

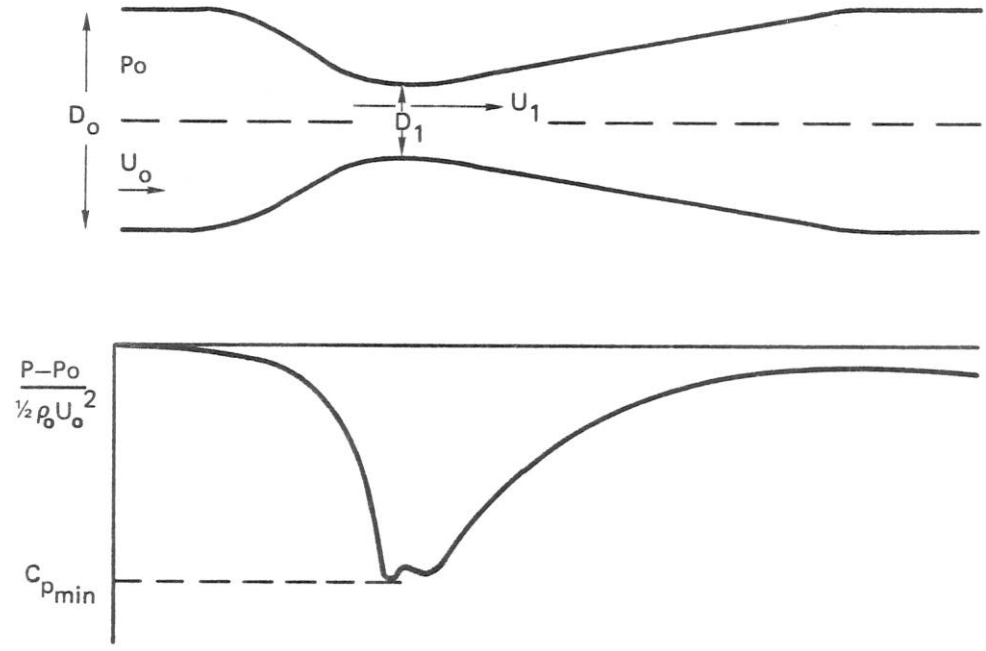

Fig. 7.25. Pressure Distribution for Flow through a Venturi Nozzle

nozzle. To a first approximation, the minimum pressure coefficient can be calculated simply by writing the Bernoulli equation for the average flow speeds,

$$p_o + \frac{1}{2}\rho_o U_o^2 \doteq p_1 + \frac{1}{2}\rho_o U_1^2 \quad , \tag{7.80}$$

and the equation of continuity,

$$U_o D_o^2 = U_1 D_1^2 \quad , \tag{7.81}$$

from which

$$\left| C_{p_{min}} \right| \doteq \frac{p_o - p_1}{\frac{1}{2}\rho_o U_o^2} \doteq \left(\frac{U_1}{U_o} \right)^2 - 1 = \left(\frac{D_o}{D_1} \right)^4 - 1 \quad . \tag{7.82}$$

Actually the critical index may be somewhat larger, because the wall pressure is lower than the

pressure at the center of the nozzle due to effects of streamline curvature; however, for a well-designed nozzle these effects are small.

If a sharp-edged orifice is used, cavitation will usually occur first downstream in violent eddies. The critical index will likely be significantly higher than that calculated using Eq. 7.82.

Valves

Valve cavitation depends not only on the construction of the valve but also on its degree of openness. Ball (1957) found that the inception index for gate valves is 0.5 when open, increasing to 1.5 when half closed and rising even higher as they are closed further. He found globe valves to be less prone to cavitation than gate valves. Clearly it is best to avoid using valves in a slightly open position. When valves are required to cause significant pressure drops, the same effect can be achieved by the use of a large number of small-diameter parallel tubes each of which is either fully open or fully shut. Multiple orifice valves have been developed for use in systems where avoidance of cavitation is considered essential, as described by Müller (1958).

Pipe Bends

At pipe bends the pressure builds up on the far wall and decreases on the inside wall. In fact, some flow meters use this pressure difference to determine the rate of flow. Critical cavitation indices of pipe bends depend upon the sharpness of the bend and vary from about 0.7 for gradual bends to about 2 for sharp ones. Kamiyama (1966) found values of 0.9 to 1.2 for 90° bends. He noted that, other things being equal, cavitation is less likely if the low-pressure region is shorter, thereby allowing less time for nuclei to grow into bubbles.

Hydraulic Machinery

Just as the propulsor is the most likely place for cavitation to occur first for propelled vehicles, so cavitation of pumps or turbines is generally the most critical in hydraulic systems. Much research has been done on this subject, primarily motivated by the need to avoid cavitation erosion and energy losses. Bashta (1961), Khoroshev (1960), Shalnev (1951) and Wislicenus (1947) have studied pump cavitation from these points of view. A detailed discussion of cavitation in hydraulic machinery is beyond the scope of the present volume. The interested reader is directed to these references and also to the next chapter on propeller cavitation, since there are many similarities between pump and propeller cavitation.

7.10 Underwater Explosions

Detonation of an explosive charge creates a small pocket of gaseous reaction products at exceedingly high temperature and pressure. This expands at transonic speed, creating a strong shock wave which propagates outward at close to the speed of sound. The initial rapid expansion caused by the detonation continues past the point of static equilibrium, the gas pressure falling well below the ambient static pressure. The unstable bubble thus created then collapses in the same manner as a large cavitation bubble, overshooting and recompressing the permanent gas. The expansion and collapse processes are then repeated until the bubble has migrated upward to the surface or has broken up into a number of smaller bubbles. Extensive research on underwater explosions carried on during World War II has been summarized in a book by Cole (1948).

Underwater explosives and explosion-like impulsive sources are being used increasingly as sources for acoustic propagation measurements and for seismic profiling in connection with off-

shore oil prospecting. As their use has increased in recent years, these pulse sources have become important contributors to low-frequency ambient noise in the oceans. The significance of explosives as noise sources can be appreciated from a simple energy analysis. Detonation of a pound of TNT releases approximately 10^7 Joules of energy. Dependent on the depth of the explosion, from 10 to 40% of this energy is radiated as sound. Thus, one 1-lb explosion every 15 minutes would release an average of about 1000 J/sec, i.e., 1 kW of continuous broadband noise. This is equivalent to an average total source pressure level of about 200 dB re 1 μPa at 1 m. Modern sources used in seismic profiling are equivalent to several ounces of TNT and are fired at intervals of 6 to 10 seconds. They therefore have average source levels of from 205 to 215 dBμPa. Comparing this with the total acoustic output of about 180 to 185 dBμPa for an average surface ship, as given in Chapter 8, it is apparent that seismic profiling by one vessel puts as much noise into the water as is emitted by from 200 to 1000 ordinary ships.

Two distinct types of sound are produced by explosions, as shown in Fig. 7.26. One is a shock wave pulse which is of very short duration and therefore produces much high-frequency energy. The other is dominantly tonal radiation by the bubble pulsations.

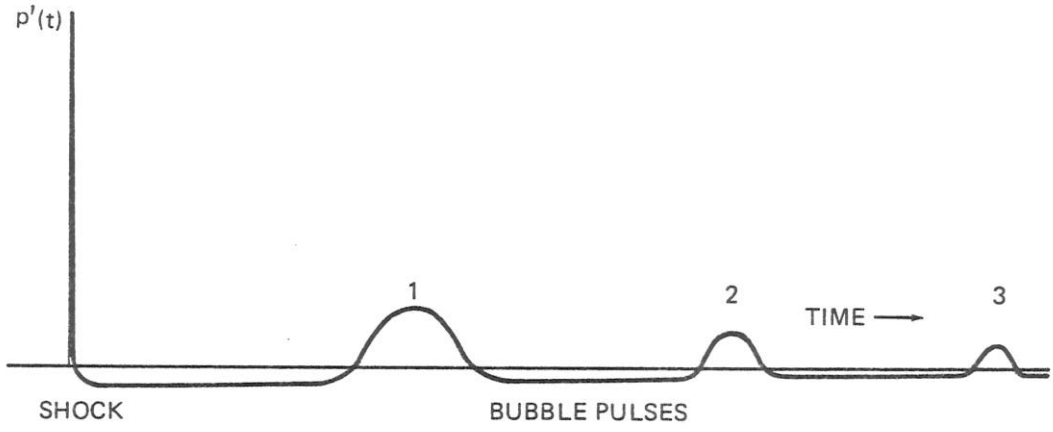

Fig. 7.26. Pressure Pulses from an Explosion, after Snay (1956)

The two parameters that characterize the shock wave pulse are its peak pressure and its duration. Both are functions of charge weight, W, and distance, r, from the point of the explosion. Arons and Yennie (1948, 1954) found that the peak pressure for TNT charges can be estimated from

$$P'_p \doteq 4 \times 10^7 \frac{W^{0.375}}{r^{1.13}} \text{ Pascals} , \tag{7.83}$$

where W is in lbs of TNT and r is distance in meters. Thus, the peak pressure is about 2.2×10^5 Pa at 100 m from a 1-lb charge. The duration of the shock-wave pulse is given by

$$\tau \doteq 0.075 W^{0.26} r^{0.22} \text{ msec} . \tag{7.84}$$

Since this time constant is often under a millisecond, the spectrum from the shock pulse is flat to over 1 kHz, decreasing 6 dB/octave at frequencies greater than τ^{-1}. Blaik and Christian (1965) have confirmed that these values are virtually unaffected by depth of the explosion.

The fundamental bubble pulse frequency is the reciprocal of the time between the shock pulse and the first bubble pulse, which time is depth dependent and is given by

$$T_o \doteq \frac{1.6W^{1/3}}{(h + 10)^{5/6}} \text{ sec} , \tag{7.85}$$

where h is the depth in meters. This relation is plotted in Fig. 7.27.

Although the peak pressure produced by the bubble pulse is independent of depth of the explosion, being given by

$$P'_B \doteq \frac{8.5 \times 10^6 W^{1/3}}{r} \text{ Pascals} , \tag{7.86}$$

the duration of the pulse is shorter at greater depths and the total bubble pulse energy therefore decreases. The bubble pulse component is suppressed if the explosion globe breaks the surface before reaching its maximum diameter or if the products can be kept within a container as is done with small charges.

In using explosions as sources, it is useful to know their spectral distributions of energy. Figure 7.28 is a plot of source spectrum levels for shallow detonations, expressed in terms of energy flux in J/m² in a 1 Hz band at 1 m. Figure 7.29 shows relative levels for 1-lb charges exploded at four deep submergences, as measured at a range of about 100 km by Kibblewhite and Denham (1970). They can be converted to source spectrum levels by adding about 50 dB to the values given.

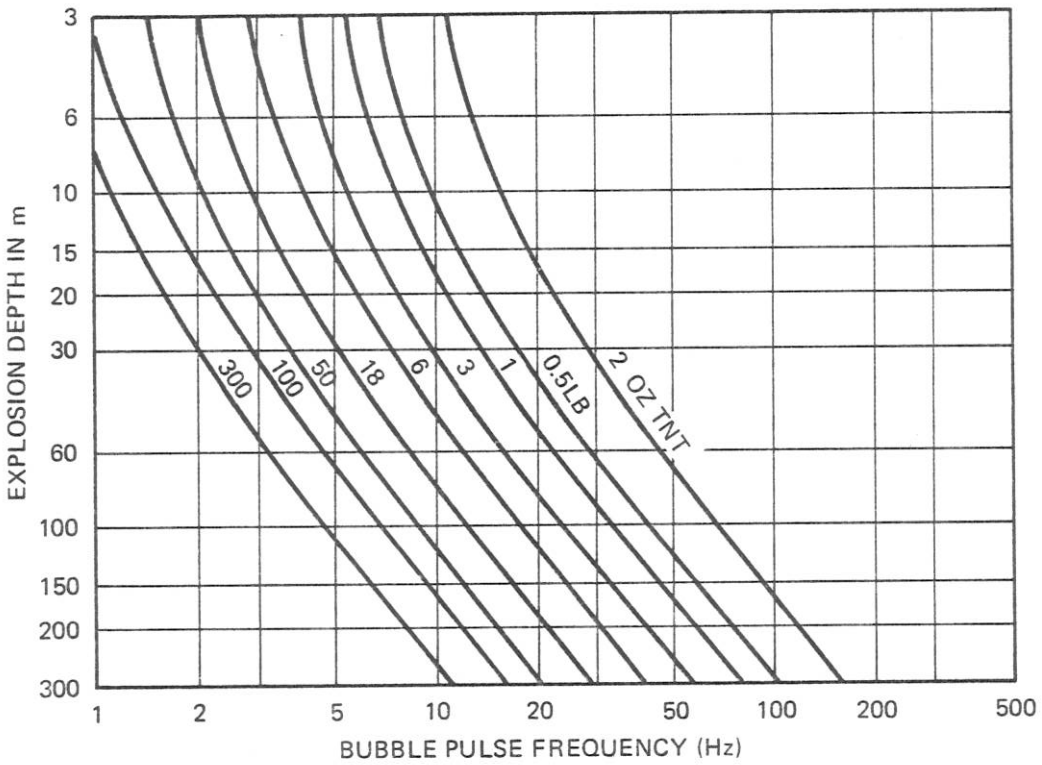

Fig. 7.27. Bubble Pulse Frequency as a Function of Depth

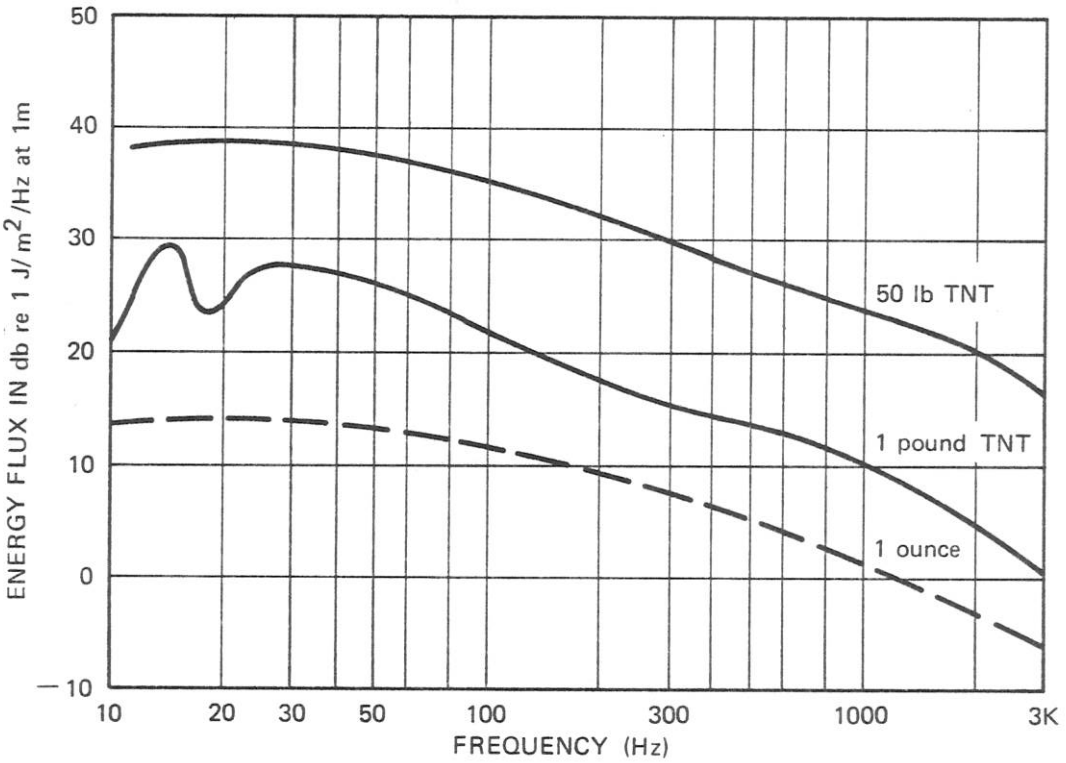

Fig. 7.28. Measured Spectra of Shallow Explosions, after Weston (1960)

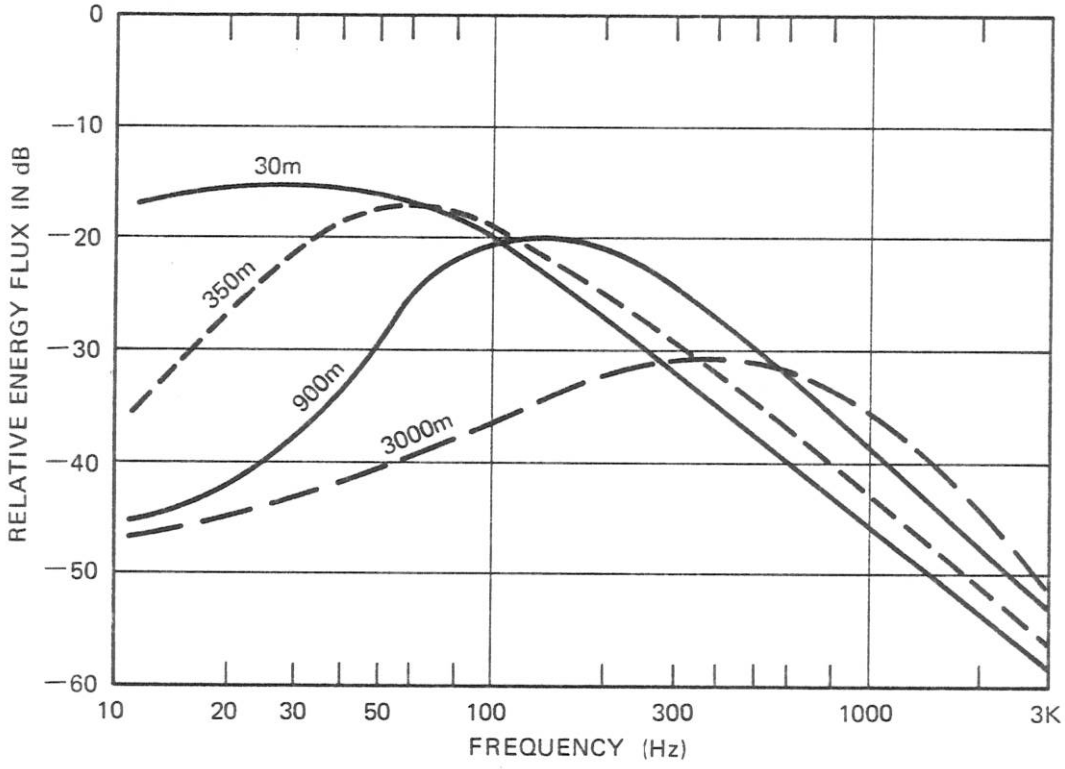

Fig. 7.29. Effect of Detonation Depth on Spectra of 1-lb Charges, after Kibblewhite and Denham (1970)

REFERENCES

Sections 7.1-7.3

Akulichev, V.A., Calculation of the cavitation strength of real liquids, *Sov. Phys.-Acoustics, 11*, 15-18, 1965.

Akulichev, V.A., Hydration of ions and the cavitation resistance of water, *Sov. Phys.-Acoustics, 12*, 144-149, 1966.

Akulichev, V.A., "Pulsations of Cavitation Voids," Part 4 of *High-Intensity Ultrasonic Fields*, L.D.Rozenberg (Ed.), Plenum Press, New York, 1971 (pp. 205-237).

Apfel, R.E., The role of impurities in cavitation threshold determination, *J.A.S.A., 48*, 1179-1186, 1970.

Bahl, S.K. and Ray, J., Collapse and expansion of a gas bubble in a liquid subject to surface tension, *Sov. Phys-Acoustics, 18*, 391-393, 1972.

Barger, J.E., Thresholds of acoustic cavitation, *Harvard Univ. Acoustics Res. Lab. Tech. Memo. 57*, April 1964.

Benjamin, T.B., "Pressure Waves from Collapsing Cavities," in *Second Symposium on Naval Hydrodynamics*, O.N.R., ACR-38, Washington, 1958 (pp. 207-229).

Benjamin, T.B. and Ellis, A.T., The collapse of cavitation bubbles and the pressures thereby produced against solid boundaries, *Phil. Trans. Royal Soc.* (London), *A260*, 221-240, 1960.

Bernd, L.H., "Cavitation, Tensile Strength, and the Surface Films of Gas Nuclei," in *Proc. Sixth Symposium on Naval Hydrodynamics*, O.N.R., ACR-136, Washington, 1966 (pp. 77-114).

Beyer, R.T., *Nonlinear Acoustics*, Naval Sea Systems Command, Washington, 1974 (Chapter 8).

Boguslavskii, Yu. Ya. and Korets, V.L., Cavitation threshold frequency dependence, *Sov. Phys.-Acoustics, 12*, 364-368, 1966.

Boguslavskii, Yu. Ya., Diffusion of a gas into a cavitation void, *Sov. Phys.-Acoustics, 13*, 18-21, 1967.

Bornhurst, W.J. and Hatsopoulos, G.N., Bubble-growth calculation without neglect of interfacial discontinuities, *J. Appl. Mech., 34*, 847-853, 1967.

Chapman, R.B. and Plesset, M.S., Nonlinear effects in the collapse of a nearly spherical cavity in a liquid, *J. Basic Engin., 94D*, 142-146, 1972.

Eisenberg, P., On the Mechanism and Prevention of Cavitation, *D.T.M.B. Repts. 712 and 842A*, July 1950 and June 1953.

Eller, A. and Flynn, H.G., Rectified diffusion during nonlinear pulsations of cavitation bubbles, *J.A.S.A., 37*, 493-503, 1965.

Eller, A.I., Growth of bubbles by rectified diffusion, *J.A.S.A., 46*, 1246-1250, 1969.

Eller, A.I., Effects of diffusion on gaseous cavitation bubbles, *J.A.S.A., 57*, 1374-1378, 1975.

Ellis, A.T., "On Jets and Shockwaves from Cavitation," in *Proc. Sixth Symposium on Naval Hydrodynamics*, O.N.R., ACR-136, Washington, Oct. 1966 (pp. 137-161).

Flynn, H.G., "Physics of Acoustic Cavitation in Liquids," Vol. I, Part B, Chapter 9 of *Physical Acoustics*, W.P. Mason (Ed.), Academic Press, New York, 1964 (pp. 57-172).

Flynn, H.G., Cavitation Dynamics: A Mathematical Formulation, *Harvard Univ. Acoustics Res. Lab. Tech. Memo. 50*, Jan. 1966.

Galloway, W.J., An experimental study of acoustically induced cavitation in liquids, *J.A.S.A., 26*, 849-857, 1954.

Gilmore, F.R., The Growth and Collapse of a Spherical Bubble in a Viscous Compressible Liquid, *C.I.T., Hydrodyn. Lab. Rept. 26-4*, April 1952. (Published in part in *Proc. Heat Transfer and Fluid Mech. Inst.*, U.C.L.A., June 1952).

Hickling, R. and Plesset, M.S., Collapse and rebound of a spherical bubble in water, *Phys. Fluids, 7*, 7-14, 1964.

Hickling, R., Some physical effects of cavity collapse in liquids, *J. Basic Engin, 88D*, 229-235, 1966.

Holl, J.W., Nuclei and cavitation, *J. Basic Engin., 92D*, 681-688, 1970.

Hsieh, D.-Y. and Plesset, M.S., Theory of rectified diffusion of mass into gas bubbles, *J.A.S.A., 33*, 206-215, 1961.

Hsieh, D.-Y., Some analytical aspects of bubble dynamics, *J. Basic Engin., 87D*, 991-1005, 1965; also, *C.I.T. Hydromech. Lab. Rept. 85-30*, April 1965.

Hsieh, D.-Y., On the dynamics of nonspherical bubbles, *J. Basic Engin., 94D*, 655-665, 1972.

Hunter, C., On the collapse of an empty cavity in water, *J. Fluid Mech., 8*, 241-263, 1960.

Iernetti, G., Cavitation threshold dependence on volume, *Acustica, 24*, 191-196, 1971.

Ivany, R.D., Hammitt, F.G. and Mitchell, T.M., Cavitation bubble collapse observations in a Venturi, *J. Basic Engin., 88D*, 649-657, 1966.

Khoroshev, G.A., Collapse of vapor-air cavitation bubbles, *Sov. Phys.-Acoustics, 9*, 275-279, 1963.

Kling, C.L. and Hammitt, F.G., A photographic study of spark-induced cavitation bubble collapse, *J. Basic Engin., 94D*, 825-833, 1972.

Knapp, R.T. and Hollander, A., Laboratory investigations of the mechanism of cavitation, *Trans. A.S.M.E., 70*, 419-435, 1948.

Knapp, R.T., Daily, J.W. and Hammitt, F.G., *Cavitation*, McGraw-Hill, New York, 1970 (Chapters 3 and 4).

Kobayashi, R., Growth and collapse of a cavity close to a solid boundary, *Repts. Inst. of High-Speed Mech.* (Japan), *18*, (173), 43-66, 1966.

Kozyrev, S.P., Cumulative collapse of vapor cavitation voids, *Sov. Phys.-Doklady, 11*, 766-768, 1966.

Kozyrev, S.P., On cumulative collapse of cavitation cavities, *J. Basic Engin., 90D*, 116-124, 1968, and *91D*, 857-858, 1969.

Lamb, Sir Horace, *Hydrodynamics*, 6th Edit., Cambridge University Press, 1932; Dover, New York, 1945 (Chapter 5).

Lauterborn, W., Photographic study of tensile strength of water using a centrifuge, *Acustica, 22*, 35-47, 1969 (in German).

Messino, D., Sette, D., and Wanderlingh, F., Statistical approach to ultrasonic cavitation, *J.A.S.A., 35*, 1575-1583, 1963.

Mitchell, T.M. and Hammitt, F.G., Asymmetrical cavitation bubble collapse, *J. Fluids Engin., 95*, 29-37, 1973.

Noltingk, B.E. and Neppiras, E.A., Cavitation produced by ultrasonics, *Proc. Phys. Soc. London, 63B*, 674-685, 1950.

Olson, H.G. and Hammitt, F.G., High-speed photographic studies of ultrasonically induced cavitation, *J.A.S.A., 46*, 1272-1283, 1969.

Plesset, M.S., The dynamics of cavitation bubbles, *J. Appl. Mech., 16*, 277-282, 1949.

Plesset, M.S., "Physical Effects in Cavitation and Boiling," Chapter 12 in *First Symposium on Naval Hydrodynamics*, Publ. 515, Nat. Acad. of Sci., Nat. Res. Coun., Washington, 1957 (pp. 297-323).

Plesset, M.S., "Bubble Dynamics," in *Cavitation in Real Liquids*, R. Davies (Ed.), Elsevier, Amsterdam, 1964 (pp. 1-18).

Plesset, M.S., Cavitating Flows, *C.I.T. Rept. 85-46*, April 1969.

Plesset, M.S., "The Tensile Strength of Liquids," in *Cavitation State of Knowledge*, J.M. Robertson and G.F. Wislicenus (Ed.), A.S.M.E., 1969 (pp. 15-25).

Plesset, M.S. and Chapman, R.B., Collapse of an initially spherical vapour cavity in the neighborhood of a solid boundary, *J. Fluid Mech., 47*, 283-290, 1971; also *C.I.T. Rept. 85-49*, June 1970.

Poritsky, H., The collapse and growth of a spherical bubble or cavity in a viscous fluid, *Proc. First U.S. Nat. Congr. on Appl. Mech.*, 1952 (pp. 813-821).

Rayleigh, Lord, On the pressure developed in a liquid during the collapse of a spherical cavity, *Phil. Mag., 34*, 94-98, 1917; also, *Scientific Papers of Lord Rayleigh*, Vol. VI, Dover, New York (pp. 504-507).

Robertson, J.M., "Cavitation Today – An Introduction," in *Cavitation State of Knowledge*, A.S.M.E., 1969 (pp. 1-9).

Safar, M.H., An acoustic method of determining the distribution of air nuclei which are responsible for cavitation in water, *J. Sound and Vibr., 9*, 308-312, 1969.

Sette, D. and Wanderlingh, F., Nucleation by cosmic rays in ultrasonic cavitation, *Phys. Rev., 125*, 409-417, 1962.

Sirotyuk, M.G., Cavitation strength of water and its distribution of cavitation nuclei, *Sov. Phys.-Acoustics, 11*, 318-322, 1965.

Sirotyuk, M.G., "Experimental Investigations of Ultrasonic Cavitation," Part 5 of *High-Intensity Ultrasonic Fields*, L.D. Rozenberg (Ed.), Plenum Press, New York, 1971 (Chapters 1 and 2).

Strasberg, M., The onset of ultrasonic cavitation in tap water, *J.A.S.A., 31*, 163-176, 1959; also, *D.T.M.B. Rept. 1078*, May 1957 (Revised Edition).

Trilling, L., The collapse and rebound of a gas bubble, *J. Appl. Phys., 23*, 14-17, 1952.

Sections 7.4 and 7.5

Akulichev, V.A. and Il'ichev, V.I., Spectral indication of the origin of ultrasonic cavitation in water, *Sov. Phys.-Acoustics, 9*, 128-130, 1963.

Akulichev, V.A. and Il'ichev, V.I., Interaction of ultrasonics waves in cavitation, *Sov. Phys.-Acoustics, 10*, 10-12, 1964.

Akulichev, V.A., et al, Radiation of finite-amplitude spherical waves, *Sov. Phys.-Acoustics, 13*, 281-285, 1963.

Akulichev, V.A. and Ol'shevskii, V.V., Statistical characteristics of cavitation phenomena, *Sov. Phys.-Acoustics, 14*, 22-26, 135-139, 1968.

Akulichev, V.A., "Pulsations of Cavitation Voids," Part 4 of *High-Intensity Ultrasonic Fields, op. cit* (pp. 239-259).

Benjamin, T.B., "Pressure Waves from Collapsing Cavities," in *Proc. Second Symposium on Naval Hydrodynamics*, O.N.R., ACR-38, Washington, 1958 (pp. 207-233).

Boguslavskii, Yu. Ya., Ioffe, A.I. and Naugol'nykh, K.A., Sound radiation by a cavitation zone, *Sov. Phys.-Acoustics, 16*, 17-20, 1970.

Fitzpatrick, H.M. and Strasberg, M., "Hydrodynamic Sources of Sound," Chapter 10 of *First Symposium on Naval Hydrodynamics*, Publ. 515, Nat. Acad. of Sci., Nat. Res. Coun., 1957 (pp. 241-280); also, *D.T.M.B. Rept. 1269*, Jan. 1959.

Harrison, M., An experimental study of single bubble cavitation noise, *J.A.S.A., 24*, 776-782, 1952; also, *D.T.M.B. Rept. 815*, Nov. 1952 (revised).

Il'ichev, V.I. and Lesunovskii, V.P., On the noise spectra associated with hydrodynamic cavitation," *Sov. Phys.-Acoustics, 9*, 25-28, 1963.

Khoroshev, G.A., Collapse of vapor-air cavitation bubbles, *Sov. Phys.-Acoustics, 9*, 275-279, 1963.

Levkovskii, Yu. L., Modeling of cavitation noise, *Sov. Phys.-Acoustics, 13*, 337-339, 1967.

Levkovskii, Yu. L., Effect of diffusion on the sound radiation from a cavitation void, *Sov. Phys.-Acoustics, 14*, 470-473, 1968.

Lyamshev, L.M., On the theory of hydrodynamic cavitation noise, *Sov. Phys.-Acoustics, 15*, 494-498, 1969.

Mellen, R.H., Ultrasonic spectrum of cavitation noise in water, *J.A.S.A., 26*, 356-362, 1954.

Mellen, R.H., An experimental study of the collapse of a spherical cavity in water, *J.A.S.A., 28*, 447-454, 1956; also, *U.S. Navy Underwater Sound Lab. Repts. 279 and 326*, 1956.

Morozov, V.P., Cavitation noise as a train of sound pulses generated at random times, *Sov. Phys.-Acoustics, 14*, 361-365, 1968.

Osborne, M.F.M., The shock produced by a collapsing cavity in water, *Trans. A.S.M.E., 69*, 253-266, 1947.

Ross, D. and McCormick, B.W., Jr., Effect of Air Content on Cavitation Noise, Report to *Eighth Amer. Towing Tank Conf.*, Oct. 1948; also, *Ord. Res. Lab. Rept. 7958-115*, Oct. 1948.

Rozenberg, L.D., "The Cavitation Zone," Part 6 of *High-Intensity Ultrasonic Fields*, L.D. Rozenberg (Ed.), Plenum Press, New York, 1971 (pp. 377-387).

Sirotyuk, M.C., "Experimental Investigations of Ultrasonic Cavitation," Part 5 of *High-Intensity Ultrasonic Fields, op. cit.* (pp. 285-339).

van Wijngaarden, L., "Linear and Nonlinear Dispersion of Pressure Pulses in Liquid-Bubble Mixtures," *Proc. Sixth Symposium on Naval Hydrodynamics*, O.N.R., ACR-136, Washington, Sept. 1966 (pp. 115-135).

Section 7.6

Bebchuk, A.S. and Rozenberg, L.D., On the problem of cavitation erosion, *Sov. Phys.-Acoustics, 3*, 95-96, 395-398, 1957; *4*, 372-373, 1958 and *6*, 496-497, 1960.

Degrois, M. and Badilian, B., Cavitation in liquids subjected to ultrasonic waves, and phenomenon of relaxation produced by ultrasound, *Comptes Rendus Acad. of Sci., 254*, 231-233, 837-839, 1213-1215, 1943-1945, 1962; also, *Acustica, 21*, 222-228, 1969; and *Ultrasonics, 4*, 38-39, 1966.

Eisenberg, P., Preiser, H.S. and Thiruvengadam, A., On the mechanisms of cavitation damage and methods of protection, *Trans. Soc. Naval Arch. and Mar. Engin., 73*, 241-286, 1965.

Elpiner, I.E., On the chemical action of ultrasonic waves, *Sov. Phys.-Acoustics, 5*, 135-146, 1959.

Elpiner, I.E., *Ultrasound: Physical, Chemical and Biological Effects*, Consultants Bureau, 1964 (Chapters 4 to 6).

Finch, R.D., Sonoluminescence, *Ultrasonics, 1*, 87-98, 1963.

Garcia, R. and Hammitt, F.G., Cavitation damage and correlations with material and fluid properties, *J. Basic Engin., 89D*, 753-763, 1967.

Golubnichii, P.I., Goncharov, V.D. and Protopopov, K.V., Sonoluminescence in various liquids, *Sov. Phys.-Acoustics, 16*, 115-117, 323-326, 1970.

Hammitt, F.G., Damage due to cavitation and sub-cooled boiling bubble collapse, *Proc. Inst. of Mech. Engin., 183*, 31-50, 1968.

Hickling, R., Effects of thermal conduction in sonoluminescence, *J.A.S.A., 35*, 967-974, 1963; also, *C.I.T. Rept. 85-21*, 1962.

Hickling, R., Some physical effects of cavity collapse in liquids, *J. Basic Engin., 88D*, 229-235, 1966.

Jarman, P., Measurements of sonoluminescence from pure liquids and some aqueous solutions, *Proc. Phys. Soc. London, 73*, 628-640, 1959.

Jarman, P.D. and Taylor, K.J., The timing of the main and secondary flashes of sonoluminescence from acoustically cavitated water, *Acustica, 23*, 243-251, 1970.

Kallas, D.H. and Lichtman, J.Z., "Cavitation Erosion," in *Environmental Effects of Polymeric Materials*, Vol. I, Interscience Publishers, 1968 (Chapter 2).

Knapp, R.T., Daily, J.W. and Hammitt, F.G., *op. cit.* (Chapters 4, 8 and 9).

Kornfeld, M. and Suvorov, L., On the destructive action of cavitation, *J. Appl. Phys., 15*, 495-506, 1944.

Kuttruff, H., Relation between sonoluminescence and acoustic cavitation in liquids, *Acustica, 12*, 230-254, 1962 (in German).

Naudé, C.F. and Ellis, A.T., On the mechanism of cavitation damage by nonhemispherical cavities collapsing in contact with a solid body, *J. Basic Engin., 83D*, 648-656, 1961.

Noltingk, B.E., "The Effects of Intense Ultrasonics in Liquids," in *Handbuch der Physik*, Vol. XI/2, 1962 (pp. 258-287).

Plesset, M.S. and Ellis, A.T., On the mechanism of cavitation damage, *Trans. A.S.M.E., 77*, 1055-1064, 1955.

Plesset, M.S., Temperature effects in cavitation damage, *J. Basic Engin., 94D*, 559-566, 1972.

Plesset, M.S., Cavitation and Cavitation Damage, *C.I.T. Rept. 85-58*, March 1973.

Shalnev, K.K., Varga, I.I. and Sebestyen, D., Investigations of the scale effects of cavitation erosion, *Phil Trans Royal Soc.* (London), *A260*, 256-266, 1966.

Sirotyuk, M.G., Effect of temperature and gas content of the liquid on cavitation processes, *Sov. Phys.-Acoustics, 12*, 67-71, 199-204, 1966.

Symposium on Erosion and Cavitation, Amer. Soc. of Testing Materials, Publ. 307, Phila., Pa. 1962.

Thiruvengadam, A., A unified theory of cavitation damage, *J. Basic Engin., 85D*, 365-376, 1963.

Thiruvengadam, A., On modeling cavitation damage, *J. Ship Res., 13*, 220-234, 1969.

Thiruvengadam, A., Cavitation erosion, *Appl. Mech. Rev., 24*, 245-253, 1971.

Thiruvengadam, A., Handbook of Cavitation Erosion, *Hydronautics Inc. Rept. 7301-1*, Jan. 1974.

West, C. and Howlett, R., Experimental measurements on cavitation bubble dynamics, *Acustica, 21*, 112-117, 1969.

Sections 7.7-7.9

Abbott, I.H. and von Doenhoff, A.E., *Theory of Wing Sections*, Dover, New York, 1959; also, *N.A.C.A. Tech. Rept. 824*, 1945.

Ackeret, J., Experimental and theoretical investigations on cavitation in water, *Appl. Mech. and Thermodyn., 1*, 1-22, 1930 (in German); trans. *N.A.C.A. Tech. Memo. 1078*, 1945, and *D.T.M.B. Trans. 20*, 1936.

Arndt, R.E.A. and Ippen, A.T., Rough surface effects on cavitation inception, *J. Basic Engin., 90D*, 249-261, 1968.

Arndt, R.E.A. and Daily, J.W., "Cavitation in Turbulent Boundary Layers," in *Cavitation State of Knowledge*, A.S.M.E., 1969 (pp. 64-86).

Ball, J.W., Cavitation characteristics of gate valves and globe valves, *Trans. A.S.M.E., 79*, 1275-1283, 1957.

Bashta, T.M., Fluid cavitation in hydraulic systems, *Russian Engin. J., 41*, (9) 5-10, 1961.

Bernd, L.H., "Cavitation, Tensile Strength and the Surface Effects of Gas Nuclei," *Proc. Sixth Symposium on Naval Hydrodynamics*, O.N.R., ACR-136, Washington, Sept. 1966 (pp. 77-114).

Borden, A., "Prediction of Cavitation Inception Speeds on Rough Hydrodynamic Bodies," *Proc. Sixth Symposium on Naval Hydrodynamics*, O.N.R., ACR-136, Washington, 1966 (pp. 183-199).

Daily, J.W., Cavitation characteristics and infinite aspect-ratio characteristics of a hydrofoil section, *Trans. A.S.M.E., 71*, 269-284, 1949.

Dean, R.B., The formation of bubbles, *J. Appl. Phys., 15*, 446-451, 1944.

Glauert, H., *The Elements of Aerofoil and Airscrew Theory*, Cambridge University Press, Cambridge, 1948.

Goldstein, S. (Ed)., *Modern Developments in Fluid Dynamics*, Clarendon Press, Oxford, 1938; Dover, New York, 1965 (Chapters 9 and 10).

Holl, J.W., The inception of cavitation on isolated surface irregularities, *J. Basic Engin, 82D*, 169-183, 1960.

Holl, J.W., An effect of air content on the occurrence of cavitation, *J. Basic Engin., 82D*, 941-945, 1960.

Holl, J.W. and Wislicenus, G.F., Scale effects on cavitation, *J. Basic Engin., 83D*, 385-398, 1961.

Holl, J.W., "The Estimation of the Effect of Surface Irregularities on the Inception of Cavitation," in *Symposium on Cavitation in Fluid Machinery*, A.S.M.E., Nov. 1965 (pp. 3-15).

Holl, J.W. and Treaster, A.L., Cavitation hysteresis, *J. Basic Engin., 88D*, 199-212, 1966.

Holl, J.W., "Limited Cavitation," in *Cavitation State of Knowledge*, J.M. Robertson and G.F. Wislicenus (Ed.), A.S.M.E., 1969.

Johnson, V.E. and Hsieh, T., "The Influence of the Trajectories of Gas Nuclei on Cavitation Inception," *Proc. Sixth Symposium on Naval Hydrodynamics*, O.N.R., ACR-136, Washington, Oct. 1966 (pp. 163-182).

Johnsson, C.A., Correlation of predictions and full-scale observations of propeller cavitation, *Int. Shipbuilding Progress, 20*, 194-210, 1973.

Jorgensen, D.W., Noise from cavitating submerged water jets, *J.A.S.A., 33*, 1334-1338, 1961; also, *D.T.M.B. Rept. 1126*, Nov. 1958.

Kamiyama, S., Cavitation tests in pipe bends, *J. Basic Engin., 88D*, 252-260, 1966.

Karelin, V.Y., *Cavitation Phenomena in Centrifugal and Axial-Flow Pumps*, Sudpromgiz, 1963 (in Russian), translated by Nat. Engin. Lab., Scotland.

Kermeen, R.W., McGraw, J.T. and Parkin, B.R., Mechanism of cavitation inception and the related scale-effects problem, *Trans. A.S.M.E., 77*, 533-541, 1955; also, *C.I.T. Rept. 21-8*, July 1952.

Kermeen, R.W., Water Tunnel Tests of NACA 4412, Walchner Profile 7 and NACA 66, -012 Hydrofoils in Noncavitating and Cavitating Flows, *C.I.T. Hydrodyn. Lab. Repts. 47-5 and 47-7*, 1956.

Khoroshev, G.A., Pump vibration caused by cavitation, *Power Machinery*, No. 4, 26-30, April 1960 (in Russian); translated by Foreign Technology Div., U.S.A.F.

Knapp, R.T., "Fluid Dynamics," Vol. 20 of *N.D.R.C. Div. 6 Summary Technical Reports*, 1945.

Knapp, R.T., Daily, J.W. and Hammitt, F.G., *op. cit.* (Chapters 1, 5, 6, 7 and 11).

Landweber, L., The Axially-Symmetric Potential Flow about Elongated Bodies of Revolution, *D.T.M.B. Rept. 761*, Aug. 1951.

Lehman, A.F. and Young, J.O., Experimental investigations of incipient and desinent cavitation, *J. Basic Engin., 86D*, 275-284, 1964.

McCormick, B.W., Jr., On cavitation produced by a vortex trailing from a lifting surface, *J. Basic Engin., 84D*, 369-379, 1962.

Mises, R. von, *Theory of Flight*, McGraw-Hill, New York, 1945 (Chapters 6, 7, 8).

Müller, E.-A., "Some Experimental and Theoretical Results Relating to the Production of Noise by Turbulence," in *Proc. Second Symposium on Naval Hydrodynamics*, O.N.R., ACR-38, Washington, 1958 (pp. 45-51).

Numachi, F., Oba, R. and Chida, I., "Effect of Surface Roughness on Cavitation Performance of Hydrofoils," in *Symposium on Cavitation in Fluid Machinery*, A.S.M.E., Nov. 1965 (pp. 16-31).

Oossanen, P. van, Profile characteristics in cavitating and non-cavitating flows, *Int. Shipbuilding Progress, 18*, 115-130, 1971.

Parkin, B.R. and Holl, J.W., Incipient-Cavitation Scaling Experiments on Hemispherical and Ogive-Nosed Bodies, *Joint C.I.T. and Ord. Res. Lab. Rept. 7958-264*, May 1953.

Pearsall, I.S., "Acoustic Detection of Cavitation (in Pumps)," Paper 14 in *Vibrations in Hydraulic Pumps and Turbines, Proc. Inst. Mech. Engin., 181, 3A*, 1-8, 1966.

Pearsall, I.S., *Cavitation*, Mills and Boon, London, 1972.

Pokrovskii, B.V. and Yudin, E.Ya., Principal noise and vibration characteristics of centrifugal pumps, *Sov. Phys.-Acoustics, 12*, 303-309, 1966.

Ross, D., Airfoil Information for Propeller Design, *Ord. Res. Lab. Rept. 7958-71*, Nov. 1947.

Rouse, H. and McNown, J.S., Cavitation and Pressure Distribution of Head Forms at Zero Angle of Yaw, *State Univ. of Iowa, Studies in Engin. Bull. 32*, 1948.

Sarpkaya, T., Torque and cavitation characteristics of butterfly valves, *J. Appl. Mech, 28*, 511-518, 1961.

Shalnev, K.K., Cavitation of surface roughnesses, *J. Tech. Phys. USSR, 21*, 206-220, 1951; trans. *D.T.M.B. Trans. 259*, Dec. 1955.

Simpson, H.C., Macaskill, R. and Clark, T.A., "Generation of Hydraulic Noise in Centrifugal Pumps," Paper 12 in *Vibrations in Hydraulic Pumps and Turbines, Proc. Inst. Mech. Engin., 181, 3A*, 84-108, 1966.

Tachmindji, A.J. and Morgan, W.B., "The Design and Estimated Performance of a Series of Supercavitating Propellers," *Proc. Second Symposium on Naval Hydrodynamics*, O.N.R., ACR-38, Washington, 1958 (pp. 489-532).

Tulin, M.P., "Supercavitating Flow Past Foils and Struts," Paper 16 in *Proc. Symposium on Cavitation in Hydrodynamics*, Nat. Phys. Lab., London, Sept. 1955.

Tulin, M.P., "Supercavitating Propellers," *Proc. Fourth Symposium on Naval Hydrodynamics*, O.N.R., ACR-92, Washington, 1962 (pp. 239-286).

Tulin, M.P., "Supercavitating Flows," in *Cavitation in Real Liquids*, R. Davies (Ed.), Elsevier, Amsterdam, 1964.

van der Meulen, J.H.J., Cavitation on hemispherical nosed bodies, *Int. Shipbuilding Progress, 19*, 21-32, 333-341, 1972.

van der Walle, F., "On the Growth of Nuclei and the Related Scaling Factors in Cavitation Inception," in *Proc. Fourth Symposium on Naval Hydrodynamics*, O.N.R., ACR-92, 1962 (pp. 357-404); also, *Int. Shipbuilding Progress, 10*, 195-204, 1963.

Widnall, S.E., The structure and dynamics of vortex filaments, *Ann. Rev. Fluid Mech., 7*, 141-165, 1975.

Wislicenus, G.F., *Fluid Mechanics of Turbomachinery*, McGraw-Hill, New York, 1947; Dover, New York, 1965 (Chapters 4 and 13).

Young, J.O. and Holl, J.W., Effects of cavitation on periodic wakes behind symmetric wedges, *J. Basic Eng., 88D*, 163-176, 1966.

Section 7.10

Akulichev, V.A., Boguslavskii, Yu. Ya., Ioffe, A.I. and Naugol'nykh, K.A., Radiation of finite-amplitude spherical waves, *Sov. Phys.-Acoustics, 13*, 281-285, 1967.

Arons, A.B. and Yennie, D.R., Energy partition in underwater explosion phenomena, *Rev. Modern Phys., 20*, 519-536, 1948.

Arons, A.B., Underwater explosion shock wave parameters at large distances from the charge, *J.A.S.A., 26*, 343-346, 1954.

Beyer, R.T., *Nonlinear Acoustics*, Naval Sea Systems Command, 1974 (Chapter 4).

Blaik, M. and Christian, E.A., Near-surface measurements of deep explosions I, Pressure pulses from small charges, *J.A.S.A., 38*, 50-56, 1965.

Christian, E.A. and Blaik, M., Near-surface measurements of deep explosions II, Energy spectra of small charges, *J.A.S.A., 38*, 57-62, 1965.

Cole, R.H., *Underwater Explosions*, Princeton University Press, Princeton, 1948; Dover, New York, 1965.

Esipov, I.B. and Naugol'nykh, K.A., Expansion of a spherical cavity in a liquid, *Sov. Phys.-Acoustics, 18*, 194-197, 1972.

Friedman, B., Theory of Underwater Explosion Bubbles, *Inst. for Math. and Mech., New York Univ.*, Sept. 1947; also in *Underwater Explosion Research*, Vol. II, O.N.R., 1950.

Herring, C., Theory of the Pulsations of the Gas Bubble Produced by an Underwater Explosion, *Nat. Def. Res. Com.*, Columbia Univ., Oct. 1941; also in *Underwater Explosion Research*, Vol. II, O.N.R., 1950.

Ioffe, A.I., Kozhelupova, N.G., Naugol'nykh, K.A. and Roi, N.A., Sound radiation from a long spark in water, *Sov. Phys.-Acoustics, 13*, 180-183, 1967.

Kibblewhite, A.C. and Denham, R.N., Measurements of acoustic energy from underwater explosions, *J.A.S.A., 48*, 346-351, 1970.

Kirkwood, J.G. and Bethe, H.A., The Pressure Wave Produced by an Underwater Explosion, *O.S.R.D. Rept. 588*, May 1942 (PB 32,182); also in *Shock and Detonation Waves*, W.W. Wood (Ed.), Gordon and Breach, New York, 1967 (pp. 1-34).

LeMéhaute, B., "Theory of Explosion-Generated Water Waves," in *Advances in Hydroscience*, Vol. 7, Academic Press, New York, 1971 (pp. 1-79).

Snay, H.G., "Hydrodynamics of Underwater Explosions," Paper 13 in *Symposium on Naval Hydrodynamics*, Nat. Acad. of Sci., Nat. Res. Coun. Publ. 515, Washington, 1956 (pp. 325-352).

Urick, R.J., *Principles of Underwater Sound for Engineers*, McGraw-Hill, New York, 1967 (Section 4.3).

Weston, D.E., Underwater explosions as acoustic sources, *Proc. Phys. Soc. London, 76*(2), 233-249, 1960.